Squeezed States of Light generation for Shot Noise limited Interferometric measurements in the next generation of Gravitational Wave detectors

Imran Khan

PhD student in Astroparticle Physics

Gran Sasso Science Institute

PhD Advisor: Prof. Viviana Fafone

Tutor: Dr. Valeria Sequino

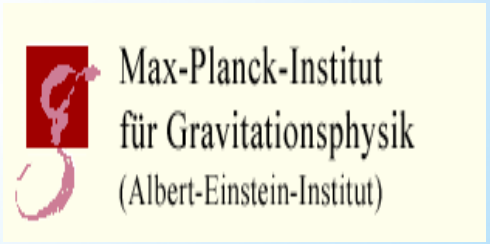

Contents

Gravitational Waves

Einstein equations

$$G_{\mu\nu} = \frac{8\pi G}{c^4} T_{\mu\nu}$$

describes how mass, that is equal to energy, bends the spacetime.

weak-field approximation

Gravitational Waves equations

$$\Box \bar{h}_{\mu\nu} = -\frac{16\pi G}{c^4} T_{\mu\nu}$$

GWs possess the properties:

- Travel at the speed of light
- Two polarizations
- Weak interaction with matter

Generated by accelerated moving bodies with a quadrupolar mass distribution

- Supernovae
- Pulsars
- Stochastic background
- Coalescent binaries

Coalescent binaries

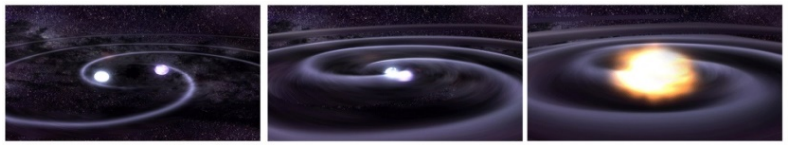

First indirect evidence of the existence of GWs: **Nobel prize 1993**: Hulse and Taylor binary system PSR 1913+16

First detection announced by the Virgo-LIGO Collaboration **on February 11, 2016,** the **Nobel prize in Physics 2017** awarded.

Direct detection of GWs

First GW detection: GW150914

Black holes of masses 36 $M_\odot$ and 29 $M_\odot$ at luminosity distance of 440 Mpc.
Final black hole mass of 62 $M_\odot$ with 3 $M_\odot$ radiated in GWs.
Transient sweeps in frequency from 35 Hz to 250 Hz with a peak strain of 1×10^{-21}.

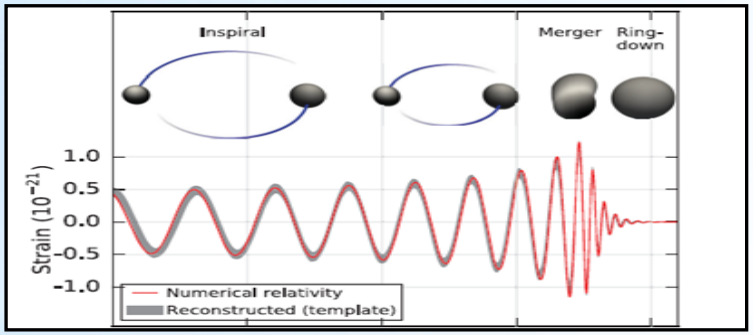

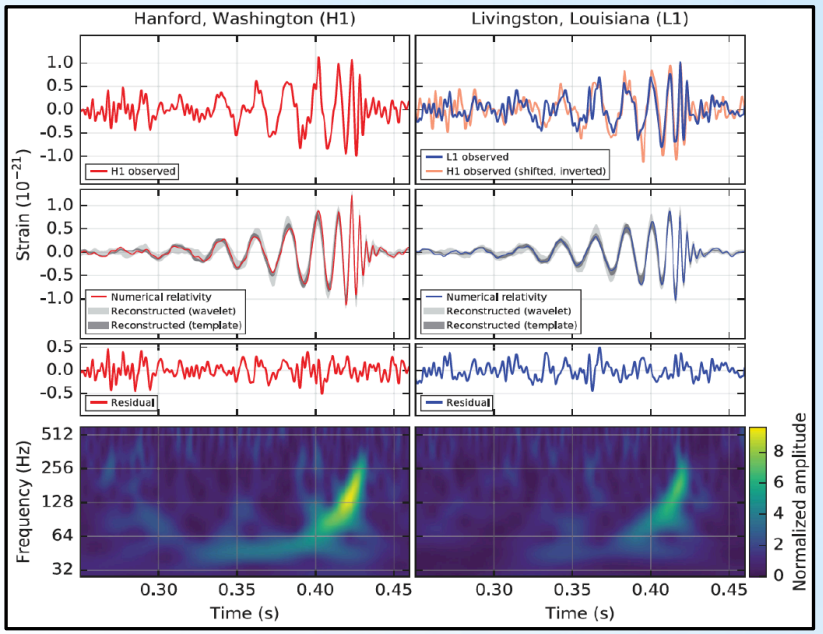

The time frequency spectrogram for all the confident detection of GWs events by the network of Advanced LIGO and AdV detectors.
GW151012, GW151226, GW170104, GW170608, GW170729, GW170809, GW170814, GW170817, GW170818, and **GW170823**

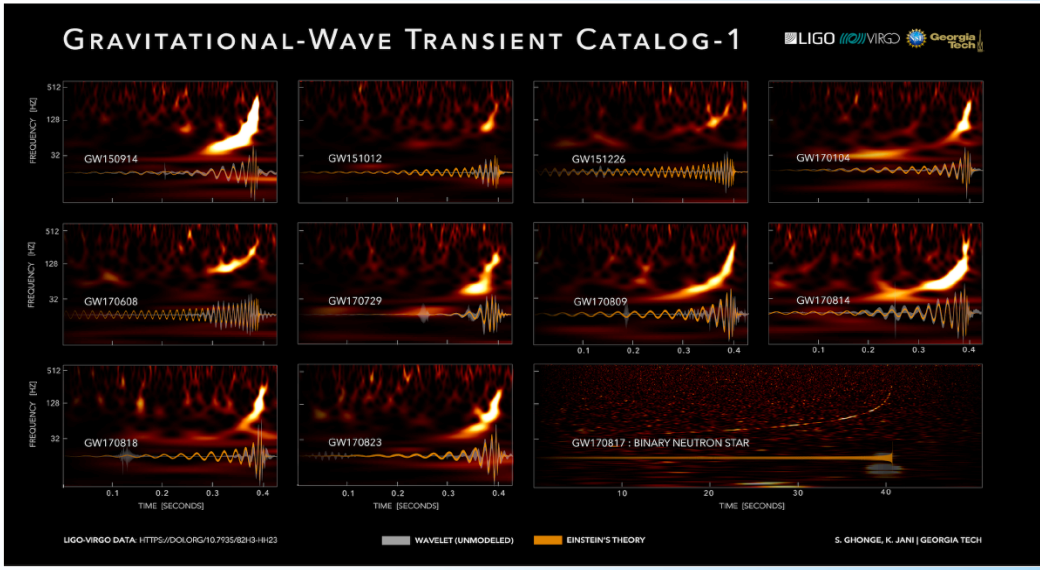

Ground based laser interferometers

Basic topology Michelson Interferometer
Sensitivity of differential length measurement to laser frequency stability can be made small.

Michelson ITF+Fabry-Perot cavities:
Increases the effective length of the interferometer.

$$\Delta\phi = \frac{4\pi}{\lambda}\Delta L = \frac{4\pi}{\lambda} h_o L_{eff}$$

$$L_{eff} = \frac{2F}{\pi} L$$

ΔL: Change in arm lengths
h: GW strain
L: Arm length

F: Finesse of Fabry-Perot cavities
At present, AdV has F = 443

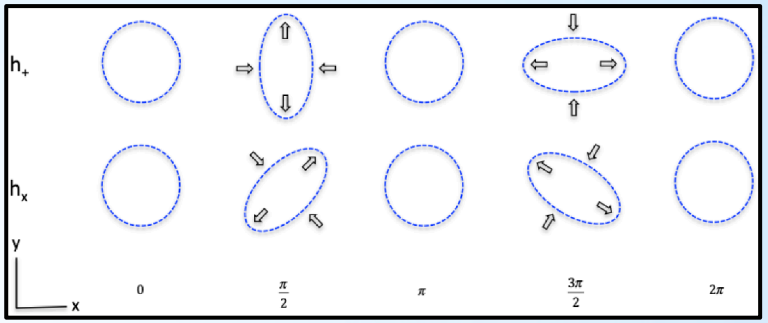

The effect of passing GWs on ring of test particles. The upper row is + polarization and the lower row is for the polarization. The different circles show different phase in the oscillation of the wave.

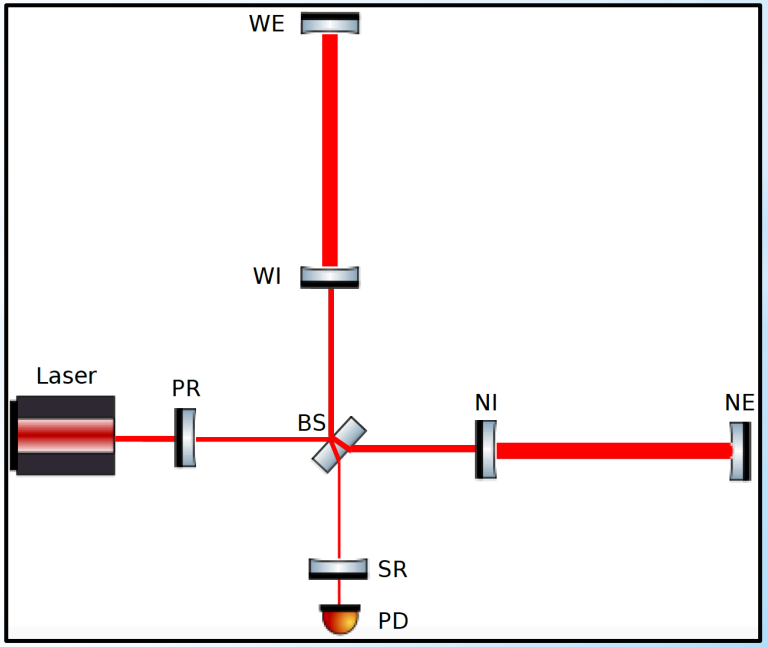

Advanced Virgo (AdV) detector

- 3 km arm length
- Sensitive to gravitational waves in the 10 to 10000 Hz frequency range
- AdV is planned to be dual recycled detector.
  - At present signal recycling cavity is not installed yet.
- Increased optical power and heavier test masses.
- French CNRS and Italian INFN collaboration
  - (Hungary, Poland, Netherland, Spain)
- Located in Cascina, Italy

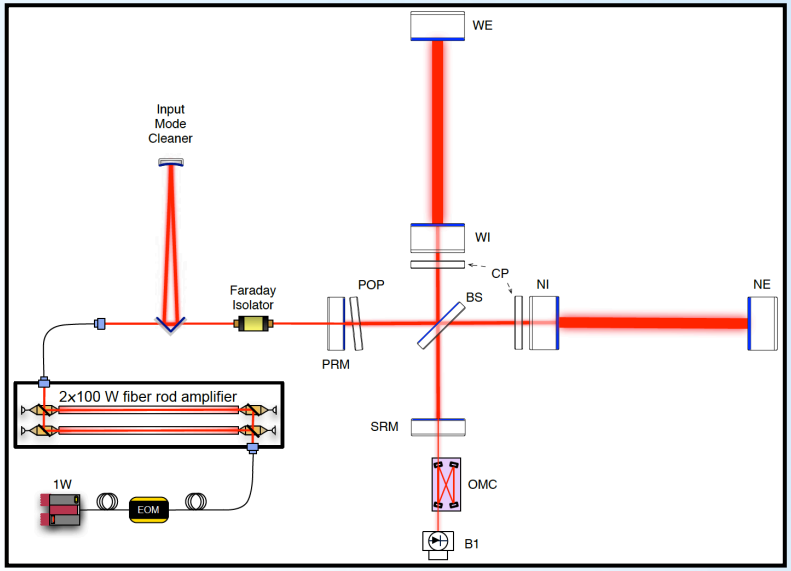

Virgo detector aerial view

Network of GW ground based detectors

Detectors network

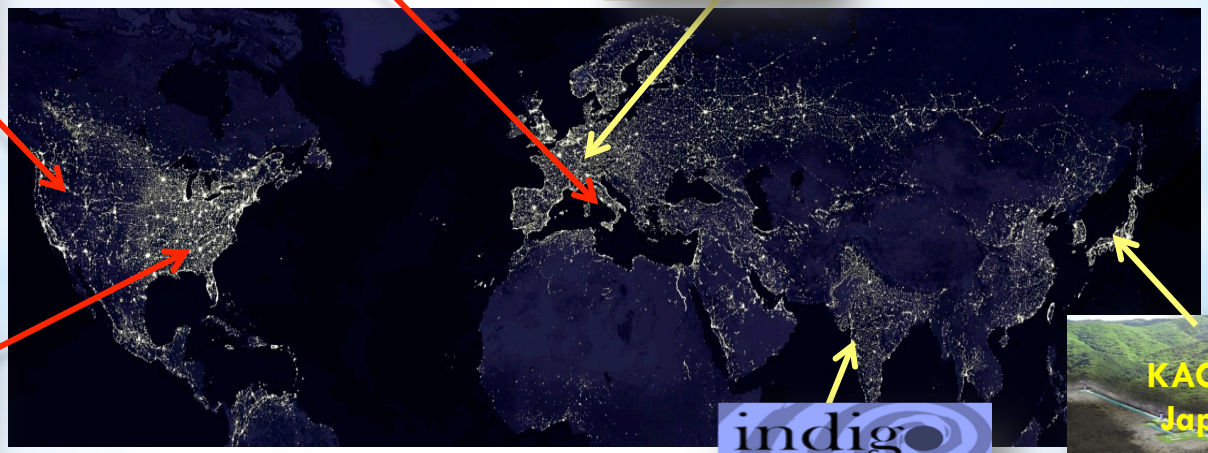

Future of Gravitational Waves Astronomy

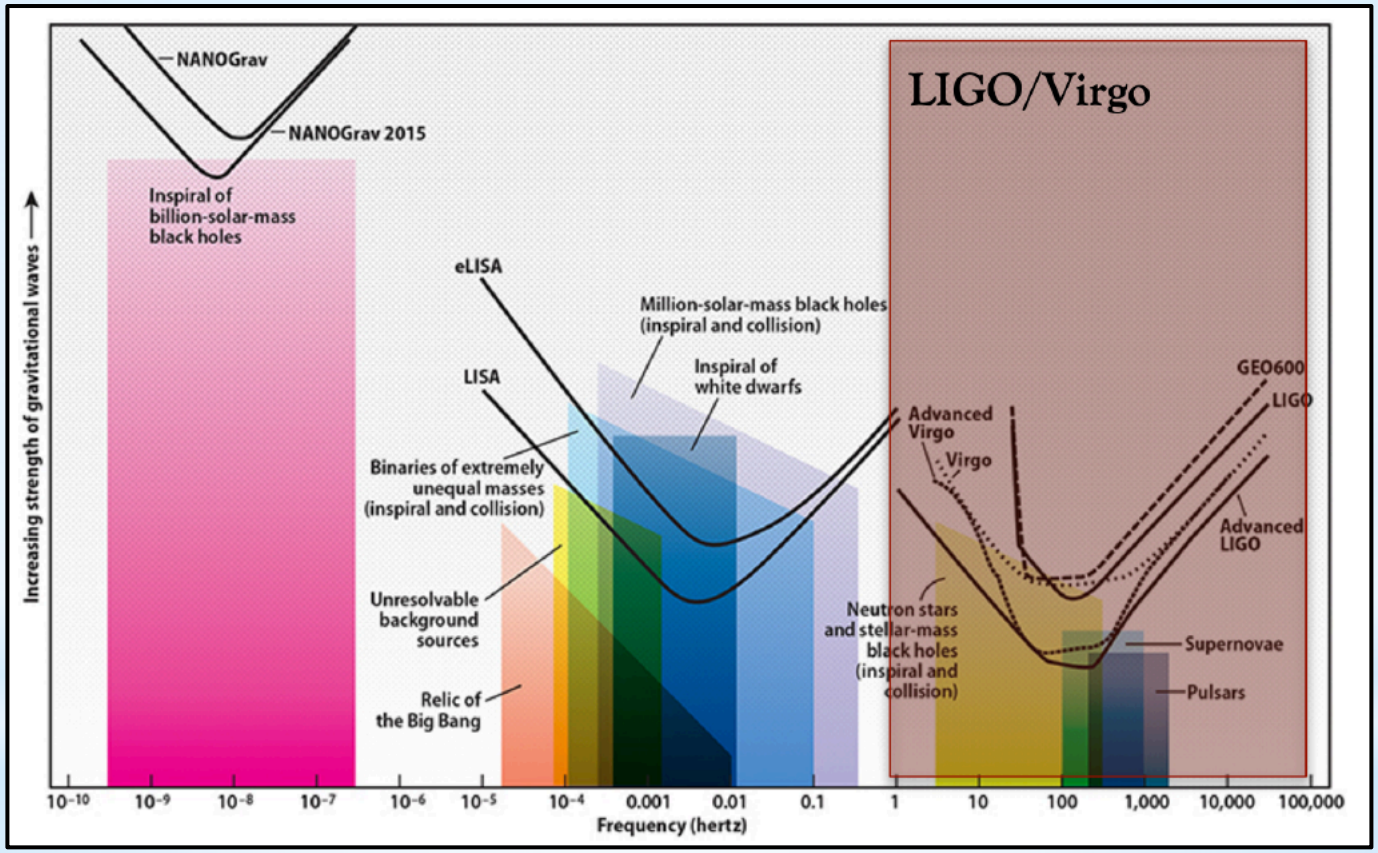

The future of Gravitational Waves astronomy with ground and space based detectors at different frequencies corresponding to different kind of astrophysical interactions. Figure credits: Roen Kelly, after C. Moore, R. Cole, and C. Berry (Institute of Astronomy, Univ. of Cambridge)

The Strain sensitivity of AdV and Noise sources

- Quantum Noise
- Gravity Gradients
- Suspension thermal noise
- Coating Brownian noise
- Coating thermo-optic noise
- Substrate Brownian noise
- Excess Gas

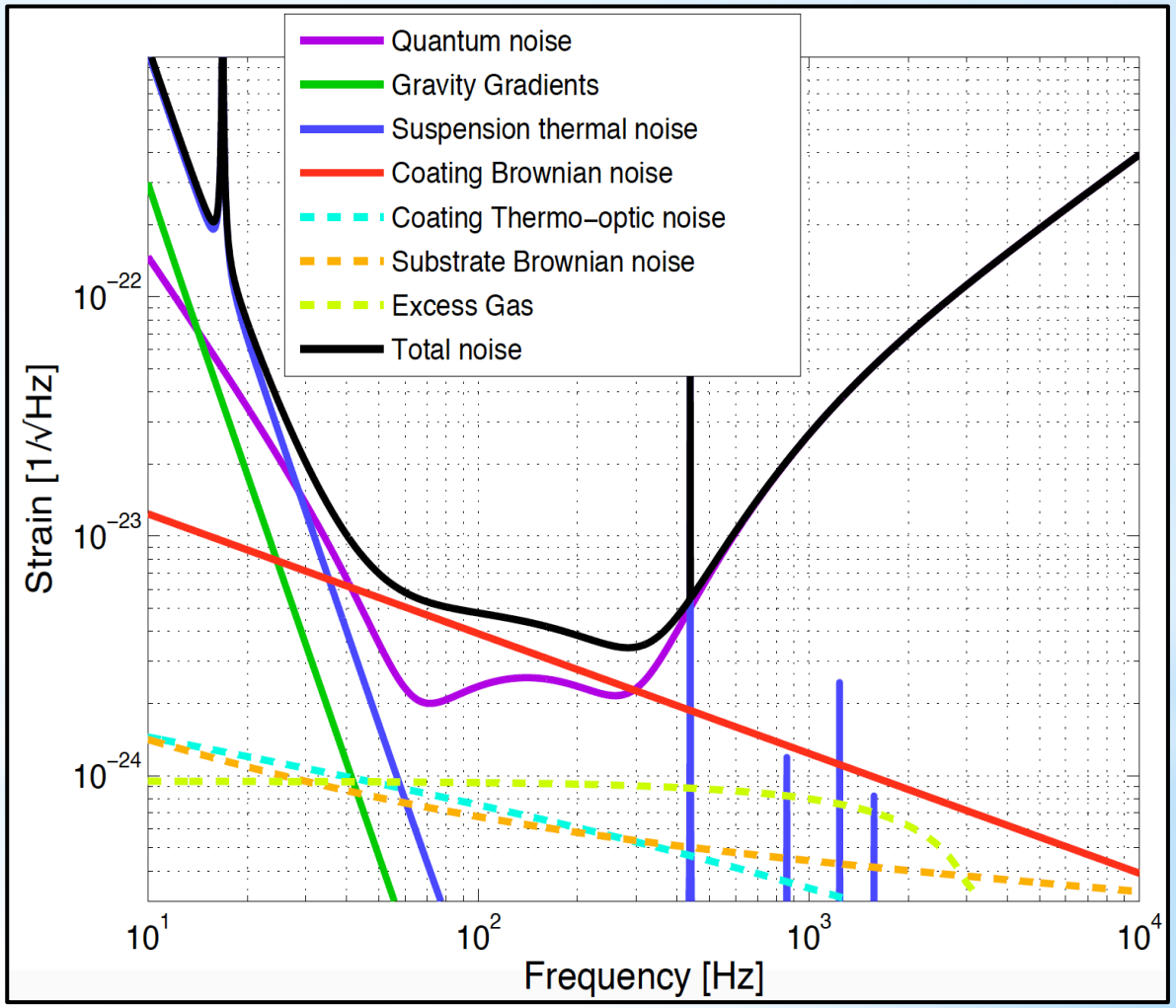

Reference AdV sensitivity and expected noise contributions

The Strain sensitivity of Virgo detector and Noise sources

- Quantum Noise
- Gravity Gradients
- Suspension thermal noise
- Coating Brownian noise
- Coating thermo-optic noise
- Substrate Brownian noise
- Excess Gas

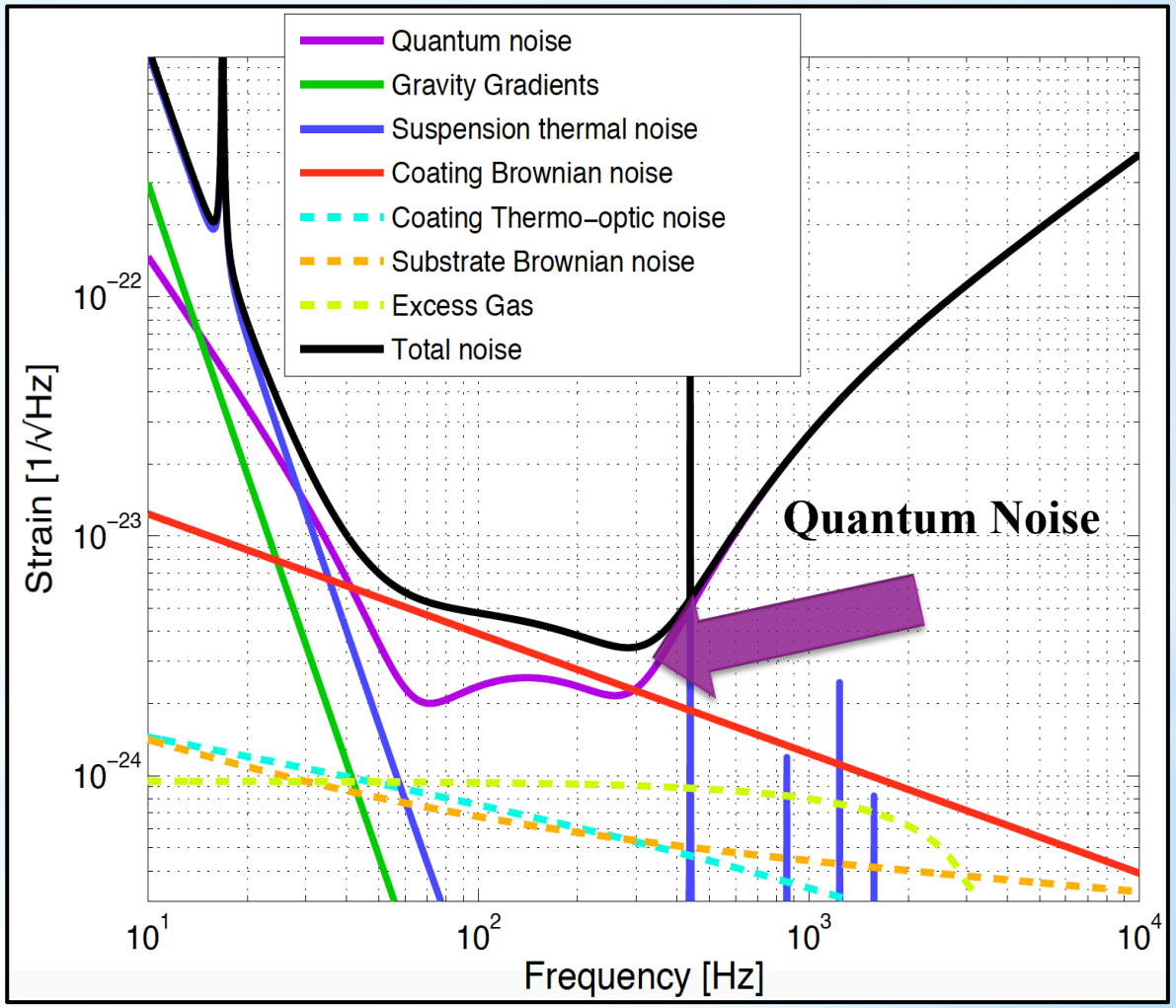

Reference AdV sensitivity and expected noise contributions

Quantum Noise

The quantum noise comprises of **Shot Noise** and **Radiation Pressure Noise**

$$\tilde{h}_{RP}(\Omega)=\frac{1}{M\Omega^2 L}\sqrt{\frac{8\pi\hbar P_{in}}{c\lambda}}$$

Quantum radiation pressure noise

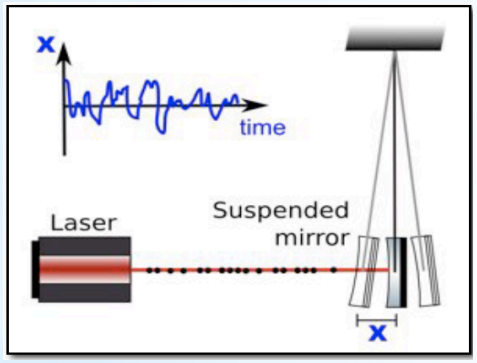

$$\tilde{h}_{shot}=\frac{1}{L}\sqrt{\frac{\hbar c\lambda}{2\pi P_{in}}}$$

Quantum shot noise

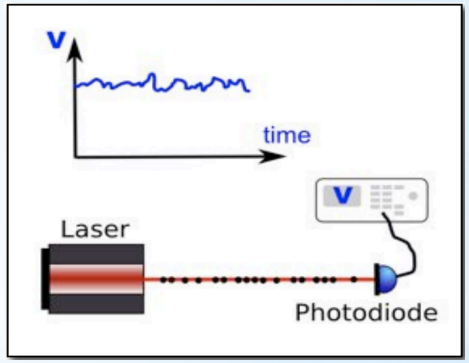

The quadrature sum of the shot noise and the radiation pressure noise

Total QN

$$h_{total}=\sqrt{h_{shot}^2(\Omega)+h_{rad}^2(\Omega)}$$

Minimizing the total quantum noise with respect to the light input power P.

SQL

$$h_{SQL}=\sqrt{\frac{4\hbar}{m\Omega^2L^2}}$$

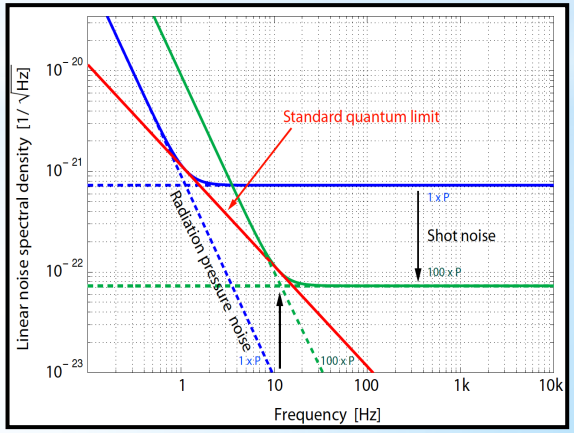

Quantized EM field

Classical EM field

Quantitative description of the electric field E at time t and position r

$$\vec{E}(\vec{r},t) = E_0\left[\vec{A}(\vec{r})e^{-iwt} - \vec{A}(\vec{r})^* e^{iwt}\right]\vec{p}(\vec{r}) \quad \text{where} \quad \vec{A}(\vec{r}) = A_0(\vec{r})e^{i\phi(\vec{r})}$$

We introduce two new properties

$$X = A^*(\vec{r}) + A(\vec{r}) \qquad \textbf{Amplitude Quadrature}$$

$$Y = i\left[A^*(\vec{r}) - A(\vec{r})\right] \qquad \textbf{Phase Quadrature}$$

So we can rewrite the classical electric field

$$\vec{E}(\vec{r},t) = E_0\left[X\cos(wt) - Y\sin(wt)\right]\vec{p}(\vec{r},t)$$

Quantum EM field

Finally introducing the quantization of the electric field

$$\hat{X} = \frac{1}{2}(a^\dagger + \hat{a}) \qquad \textbf{Amplitude Quadrature operator}$$

$$\hat{Y} = \frac{1}{2}i(\hat{a}^\dagger - \hat{a}) \qquad \textbf{Phase Quadrature operator}$$

Quantized EM field

$$\hat{\vec{E}}(\vec{r},t) = E_0\sin(kz)\left[\hat{X}\cos(wt) - \hat{Y}\sin(wt)\right]$$

Coherent and squeezed fields

Quadrature variances $\Delta\hat{X}' = e^{-r}$, $\Delta\hat{Y}' = e^{r}$

The phase space representation of the coherent and squeezed fields. The circles and the ellipses at the centre of the axis represent vacuum fields while the circles and the ellipses in X-Y plane represent bright fields.

Vacuum state under squeeze and displacements operators $|\alpha,\epsilon\rangle = D(\alpha)S(\epsilon)\,|0\rangle$

Heisenberg uncertainty principle:

there is a minimal area of the coherent state

$$\Delta\hat{X}\,\Delta\hat{Y} \geq 1$$

Phase space representation of the coherent and squeezed fields

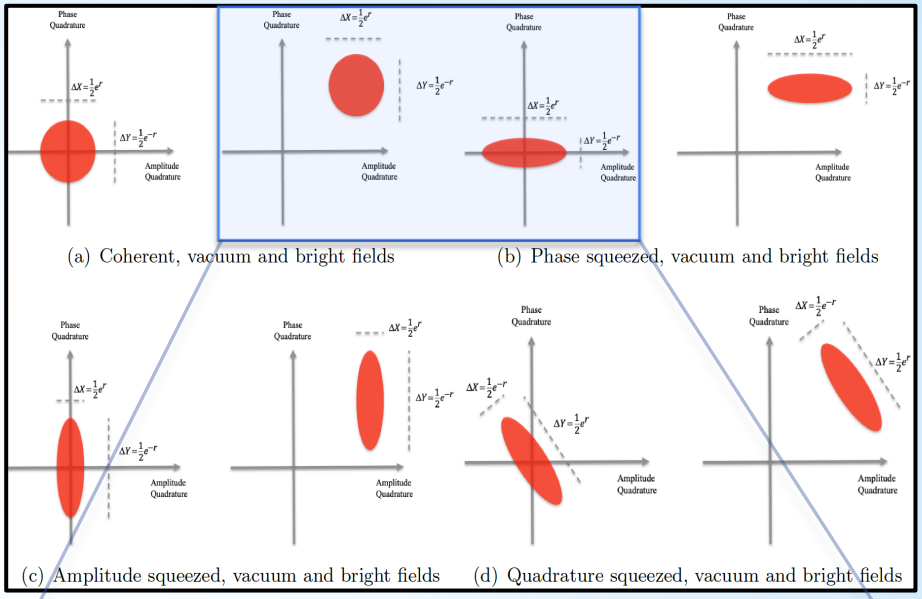

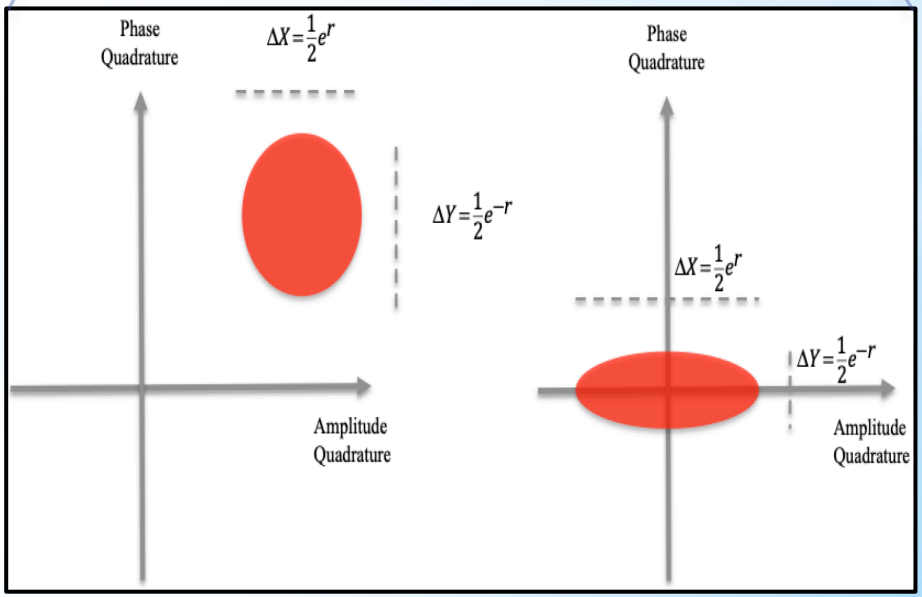

Quantum noise limited interferometric measurement

Coherent vacuum field entering from the output port of the interferometer.

It is reflected from the interferometer and detected along with the GW signal.

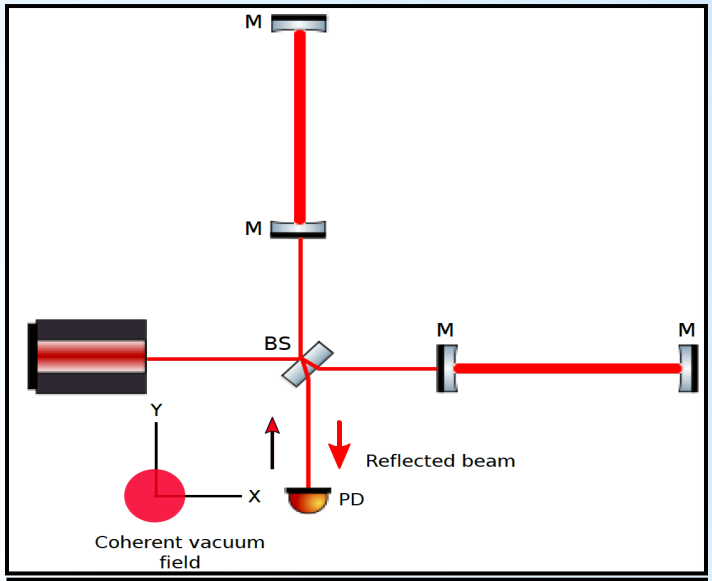

Phase squeezed vacuum field is injected from the output port of the interferometer, thus minimizing the quantum noise limited interfero-metric measurement.

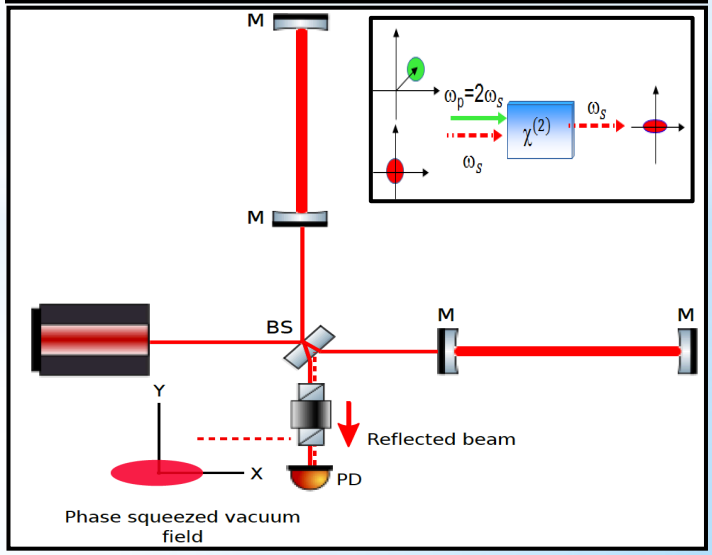

Nonlinear optics: Boyd&Kleinman theory

Theory

For a nonlinear material, the induced polarization in response to an electric field, not only linearly depends on the applied electric field but also on the higher order terms.

$$P_i = \epsilon_0(\chi_{ij}^{(1)} E_j + \chi_{ijk}^{(2)} E_j E_k + \chi_{ijkl}^{(3)} E_j E_k E_l + ...)$$

Second harmonic generation (Boyd&Kleinman theory)

$$P_{2\omega} = \frac{16\pi^2 d_{eff}^2}{\epsilon_0 c \lambda_1^3 n_3 n_1} P_\omega^2 e^{-\alpha' l} l h(\sigma, \beta, \kappa, \xi, u)$$

phase mismatch parameter

$$\sigma = \frac{1}{2} b \Delta k \qquad \Delta k = 2k_\omega - k_{2\omega}$$

focusing parameter

$$\xi = l/b \qquad b = w_0^2 k_\omega$$

The conversion efficiency η = $P_{2\omega}/P_\omega$

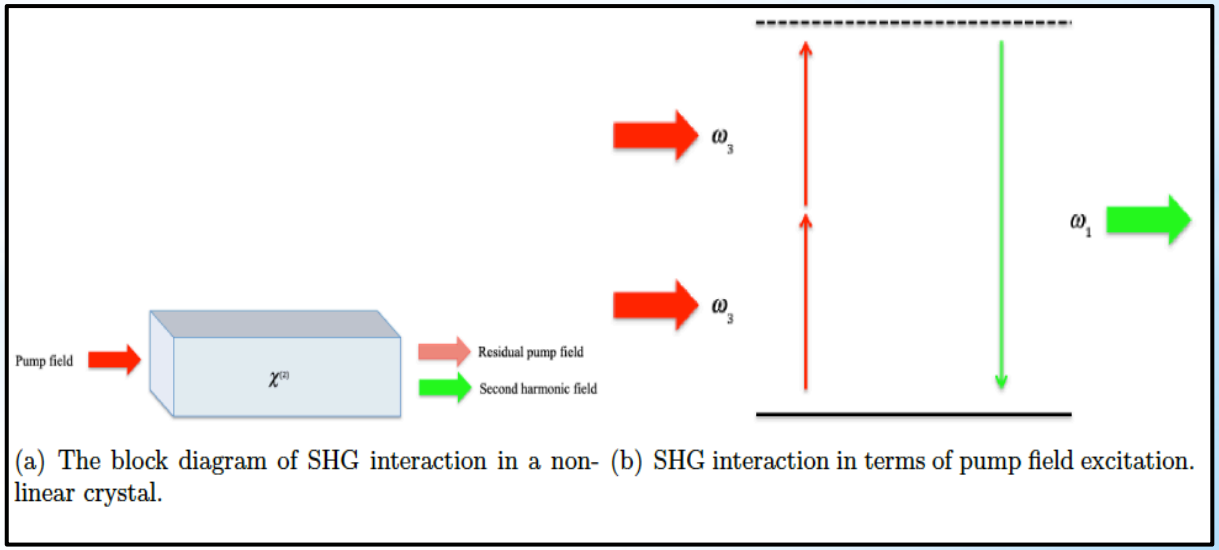

(a) The block diagram of SHG interaction in a non-linear crystal. (b) SHG interaction in terms of pump field excitation.

Nonlinear optics: Phase matching condition

Phase matching (PM) for second harmonic generation

The efficient generation of second harmonic EM wave from a nonlinear crystal needs the phases of the polarization wave and EM wave at 2ω to be the same.

The relative phase difference between the waves over one coherence length l_c

$$\Delta k l_c = \pi$$

$$l_c = \frac{\pi}{\Delta k} = \frac{\lambda_1}{4(n_2 - n_1)}$$

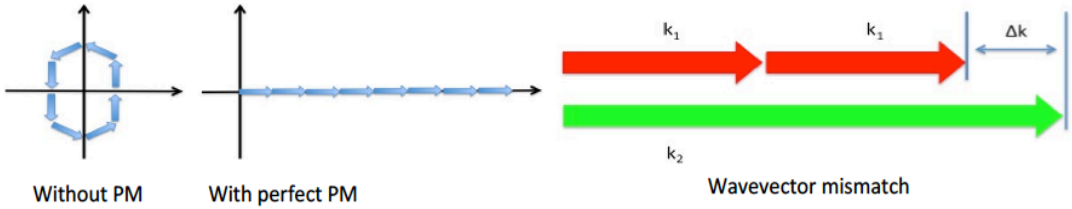

Quasi phase matching is a technique which allows the positive flow of energy from fundamental frequency to second harmonic frequency, independent of the fact that the two frequencies are not phase locked with one another. This technique allows for positive flow of energy from pump to signal and idler for the phase difference between the two frequencies until less than 180 degrees.

The interacting process of the fundamental and second harmonic waves is described by three wave coupled equations

Second harmonic output field in QPM is

$$E_{SHG}(L_{out}) = \frac{1}{m\pi}\frac{ik_{2\omega}}{n_{2w}^2}\chi^{(2)}E_1^2(0)L_{out}$$

Second harmonic output field in a perfectly phase matched case is

$$E_{SHG}(L) = \frac{ik_{2\omega}}{n_{2w}^2}\chi^{(2)}E_1^2(0)L$$

By comparing the two equations, output SHG field is $= \frac{m}{2\pi}E_{SHG}(L)$

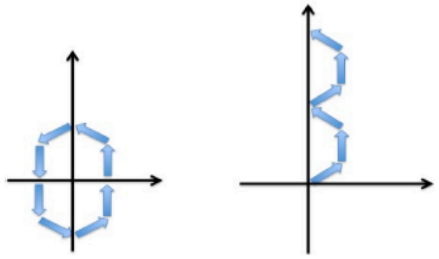

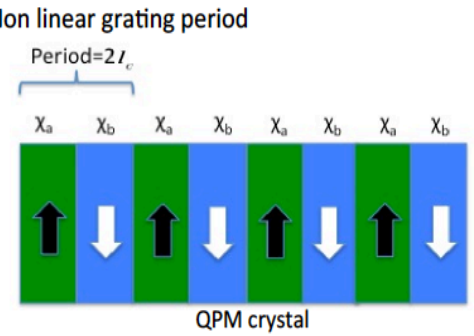

m is the order of QPM

Squeezing pump beam: Single pass SHG (at Albert Einstein Institute Hannover, Germany)

SHG in PPKTP

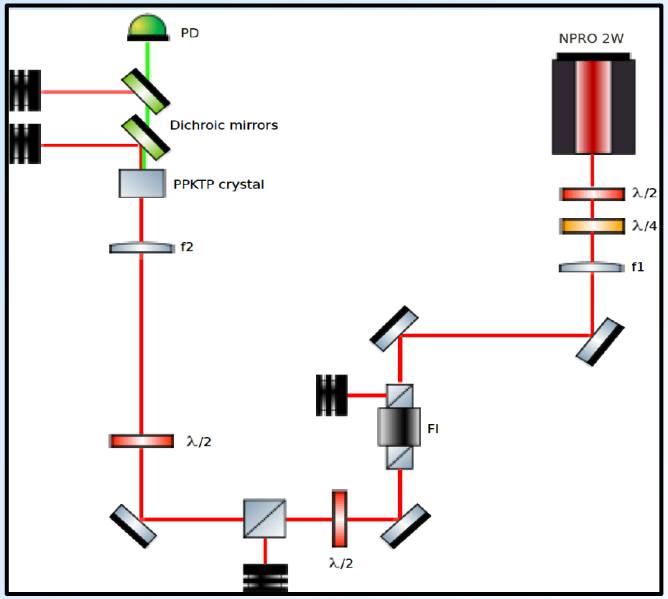

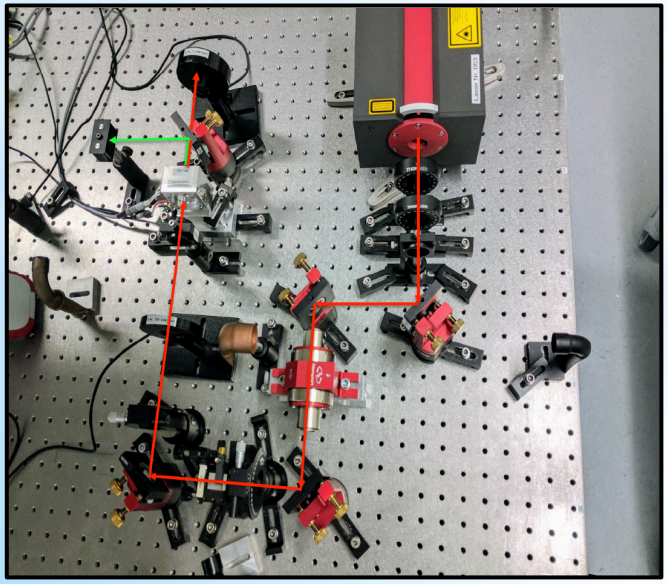

Single pass SHG in 12 mm long PPKTP crystal could possibly be used as alternate to in-cavity SHG for squeezing pump beam generation

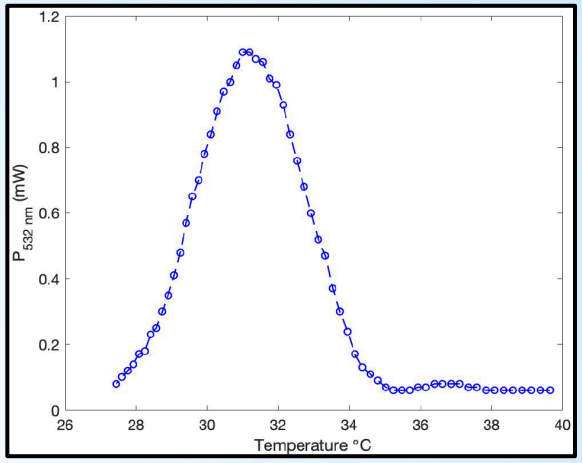

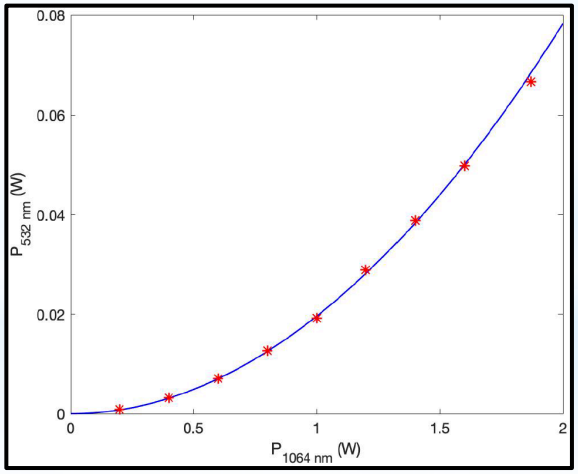

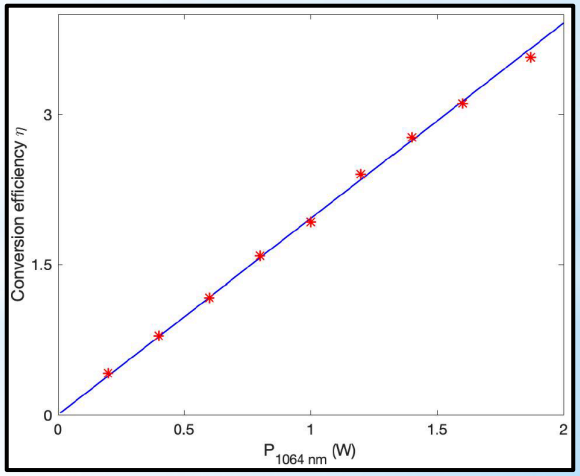

We measured up to 67 mw of light at 532 nm for 1.870 W of IR light at 1064 nm in single pass configuration

Auxiliary Lasers for AdV

Degrees of freedom (DOFs) of AdV

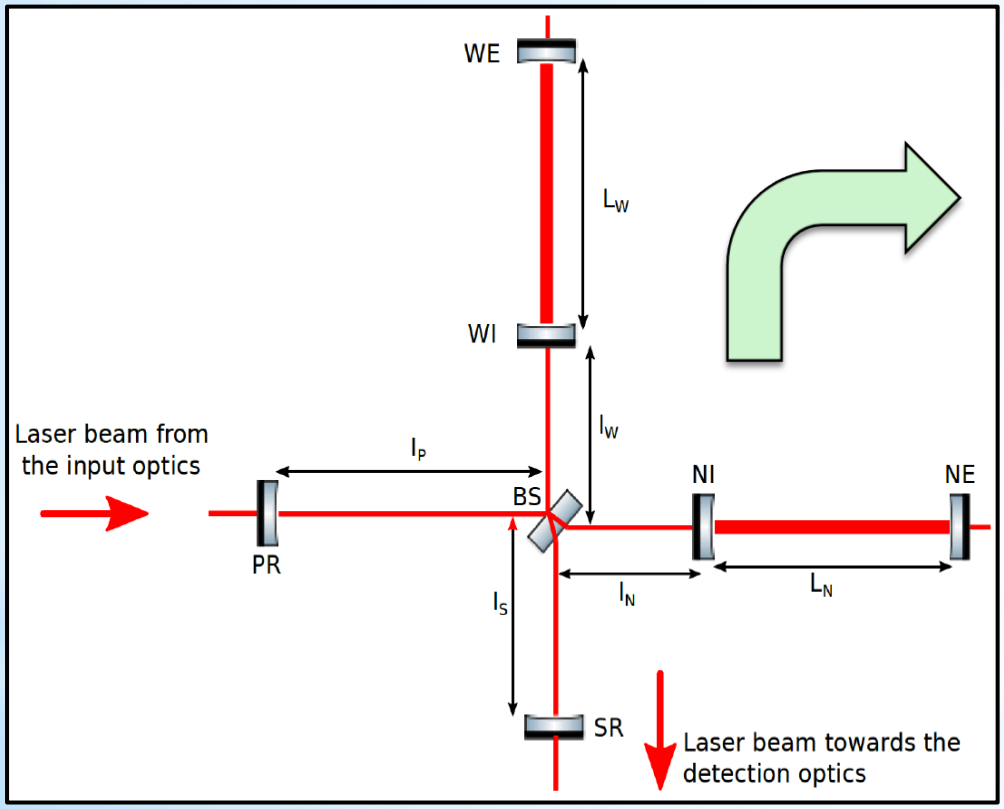

Degrees of freedom of AdV

1) Differential arm cavity length (DARM)
2) Common arm cavity length (CARM)
3) Michelson (MICH)
4) Power recycling length (PRCL)
5) Signal recycling length (SRCL)

$$DARM = \frac{L_N - L_W}{2}$$
$$CARM = \frac{L_N + L_W}{2}$$
$$MICH = l_N - l_W$$
$$PRCL = l_P + \frac{l_N + l_W}{2}$$
$$SRCL = l_S + \frac{l_N + l_W}{2}$$

DOF	Power recycled 25W	Dual recycled 25W	Dual recycled 125W
DARM	$6 \times 10^{-16} m$	$2 \times 10^{-15} m$	$1 \times 10^{-15} m$
Frequency		7 mHz	
CARM		$4 \times 10^{-13} m$	
MICH	$2 \times 10^{-13} m$	$6 \times 10^{-13} m$	$3 \times 10^{-13} m$
PRCL		$2 \times 10^{-11} m$	
SRCL			$3 \times 10^{-13} m$

As the error signal for each degree of freedom is only mildly decoupled from the others, it is too difficult to reach the working point of the interferometer controlling each degree of freedom with the same laser source at 1064 nm

Figure. Scheme of relevant physical distances between mirrors in dual recycled configuration and the required accuracy requirements for control loops of Virgo detector at main laser wavelength i.e., 1064 nm.

Virgo detector locking with auxiliary lasers

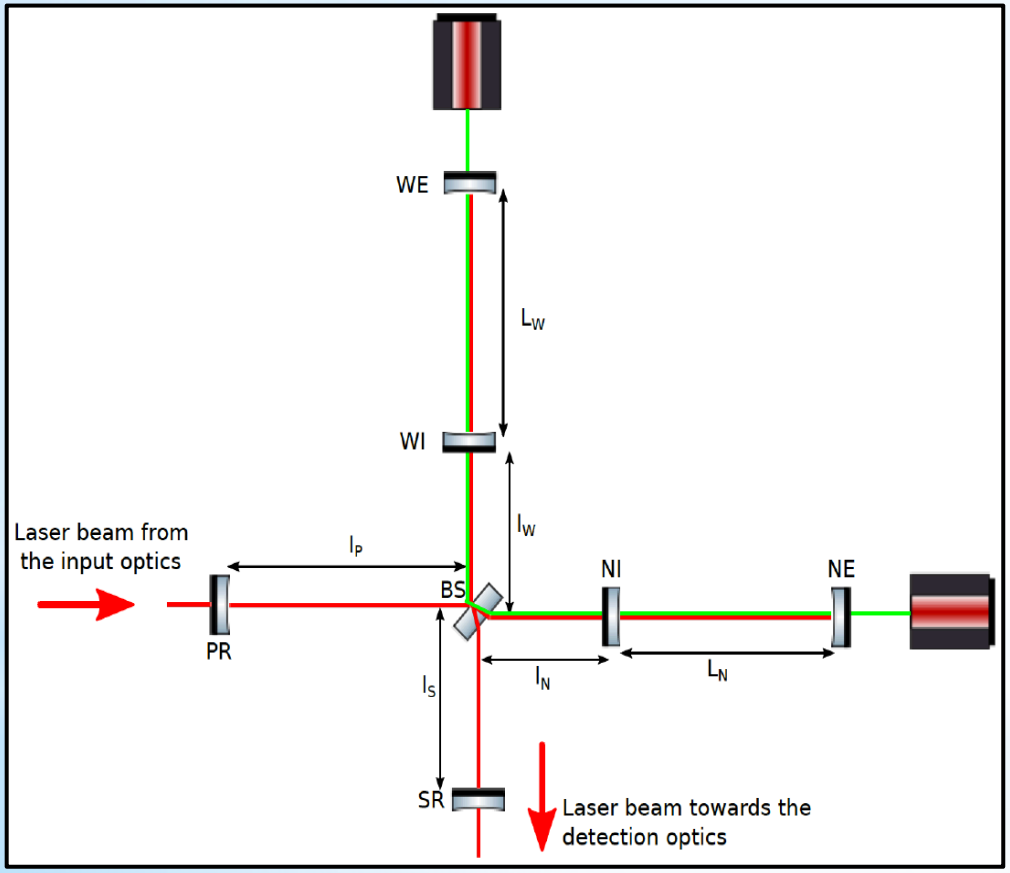

Figure. AdV locking in the presence of auxiliary lasers

The idea is lock each arm cavity individually using auxiliary lasers, at a different wavelength with respect to the main laser but phase locked to the main laser. Auxiliary lasers can control the degrees of freedom DARM and CARM with these green lasers.

Two solutions to the problem

(1) Two new laser sources
(the optical phase locked loop setup for each laser (costly solution)

(2) An all fibered green laser source
Fibered amplified IR laser source at 1064 nm to generate 532 nm in SHG.
Fibered system: ease of alignment, cost effective
no need for OPLL
Future perspective: the in-vacuum squeezing realization would depend on light transmission through optical fibers

Experiment layout: Single pass SHG in PPLN

100 mW laser source at 1064 nm

5 W laser source at 1064 nm

97 mW laser source at 532 nm

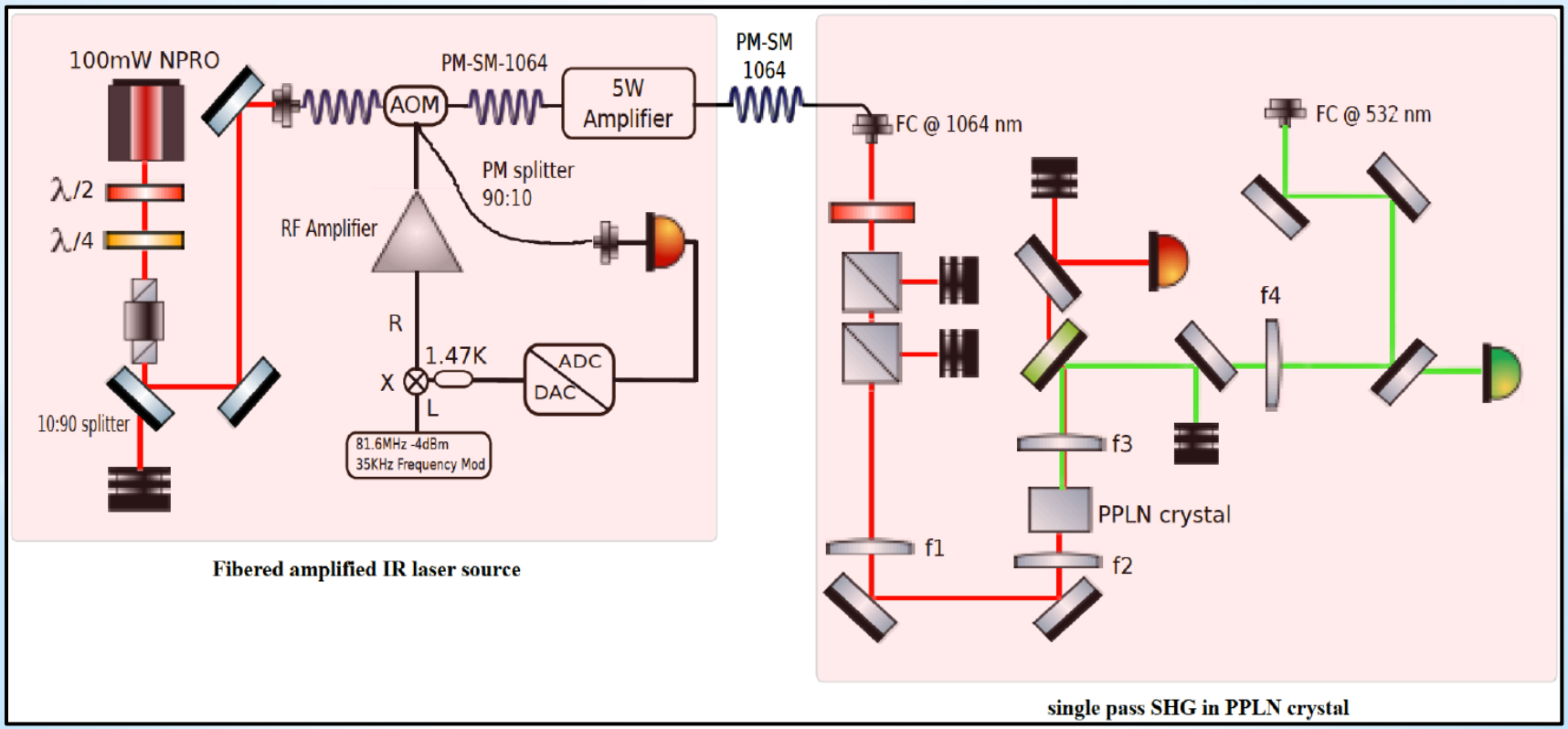

PM: Polarization maintaining
SM: Single mode

Optical bench for auxiliary lasers generation

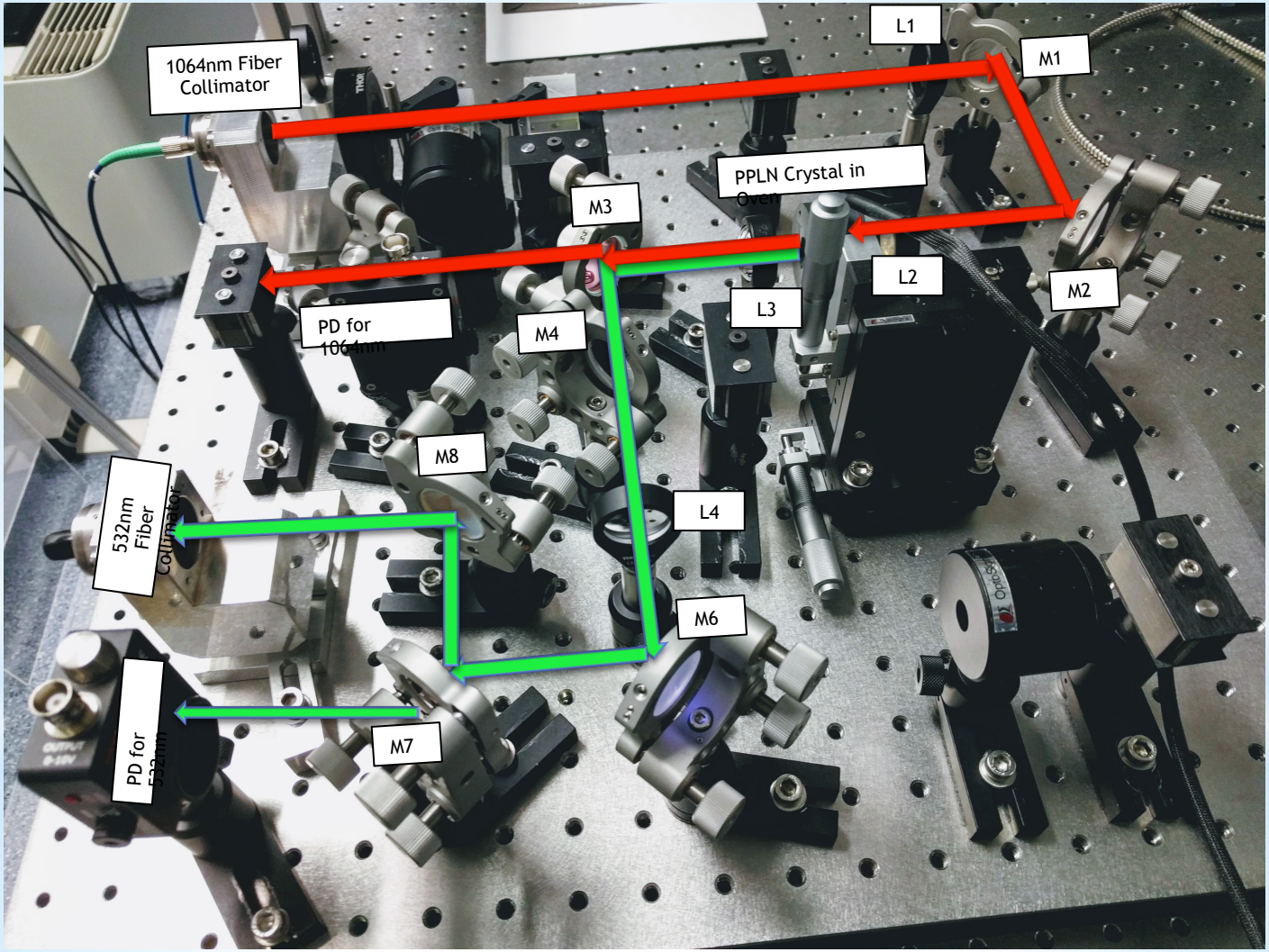

Optical bench with fundamental and second harmonic laser beams

Green laser beam on the bench

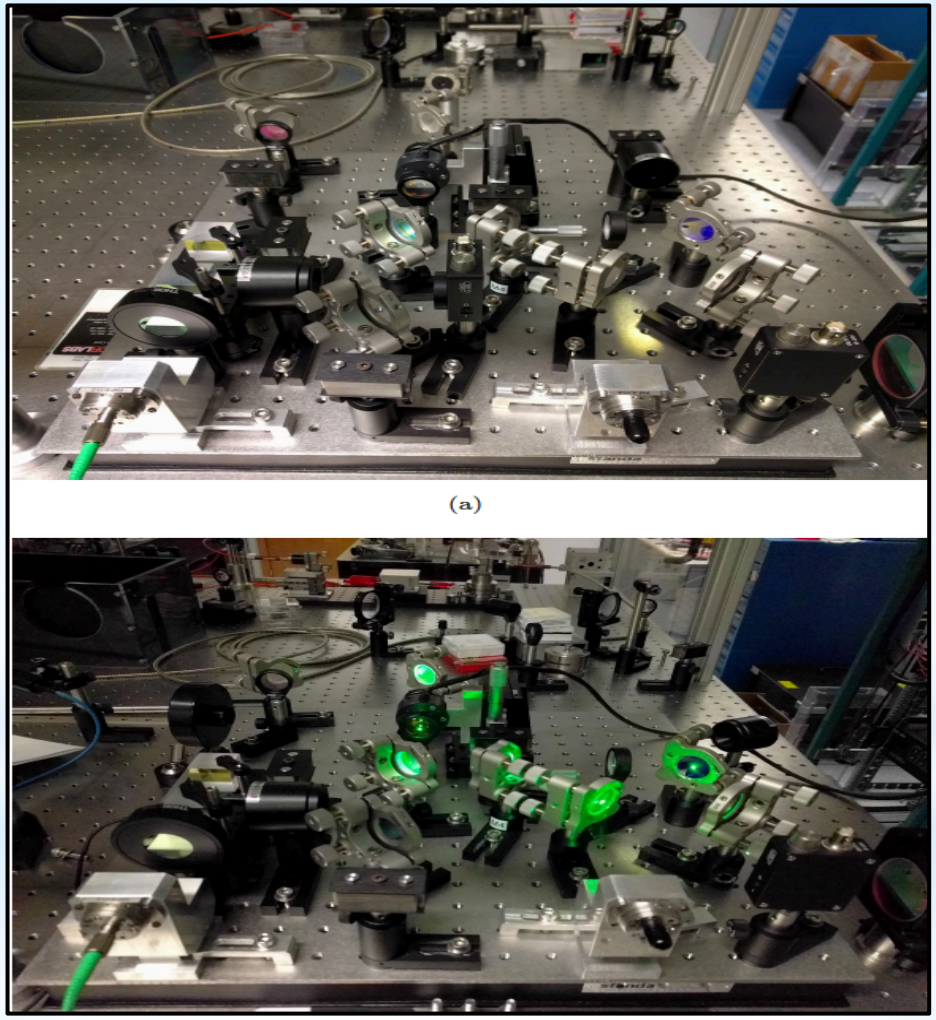

(a)

Single pass SHG optical bench. **a** without the SH beam generation, **b** with the SH beam generation.

Results

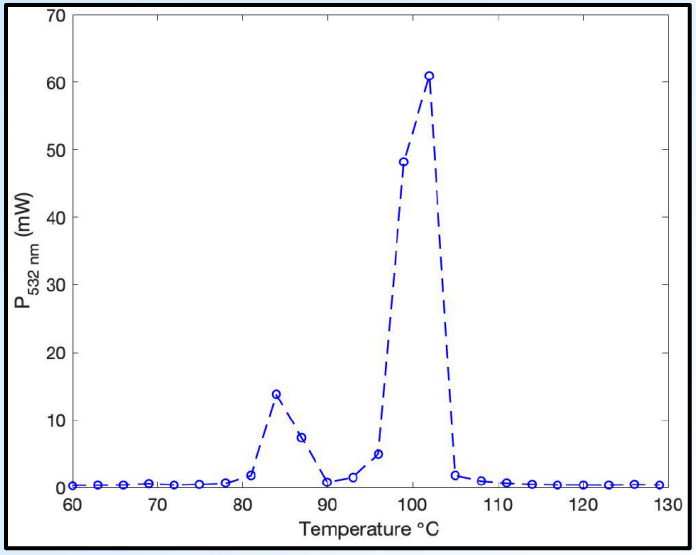

Single pass SHG at different optical powers of fundamental laser beam of waist size 20 μm inside PPLN crystal.

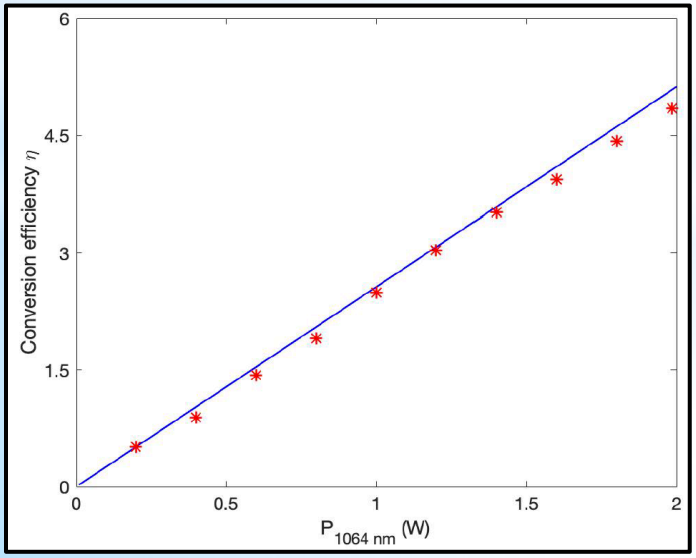

Phase matching temperature for optimum conversion efficiency of SHG interaction in PPLN crystal.

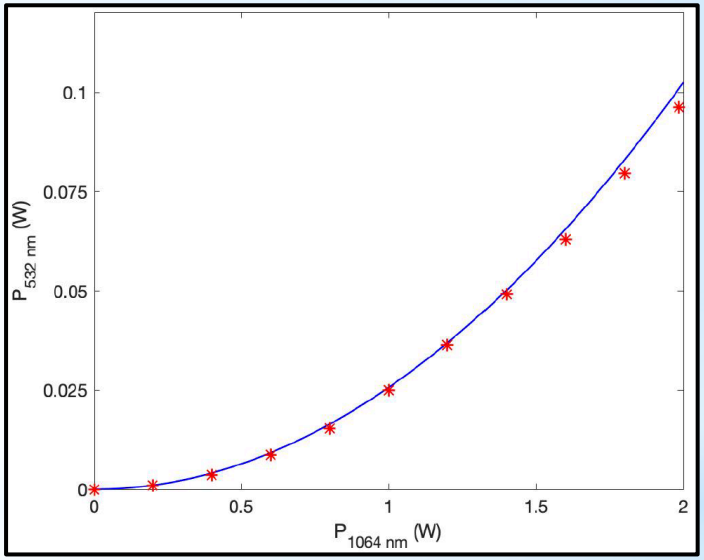

Single pass SH conversion efficiency **versus** fundamental laser beam power in PPLN crystal

Laser power stability

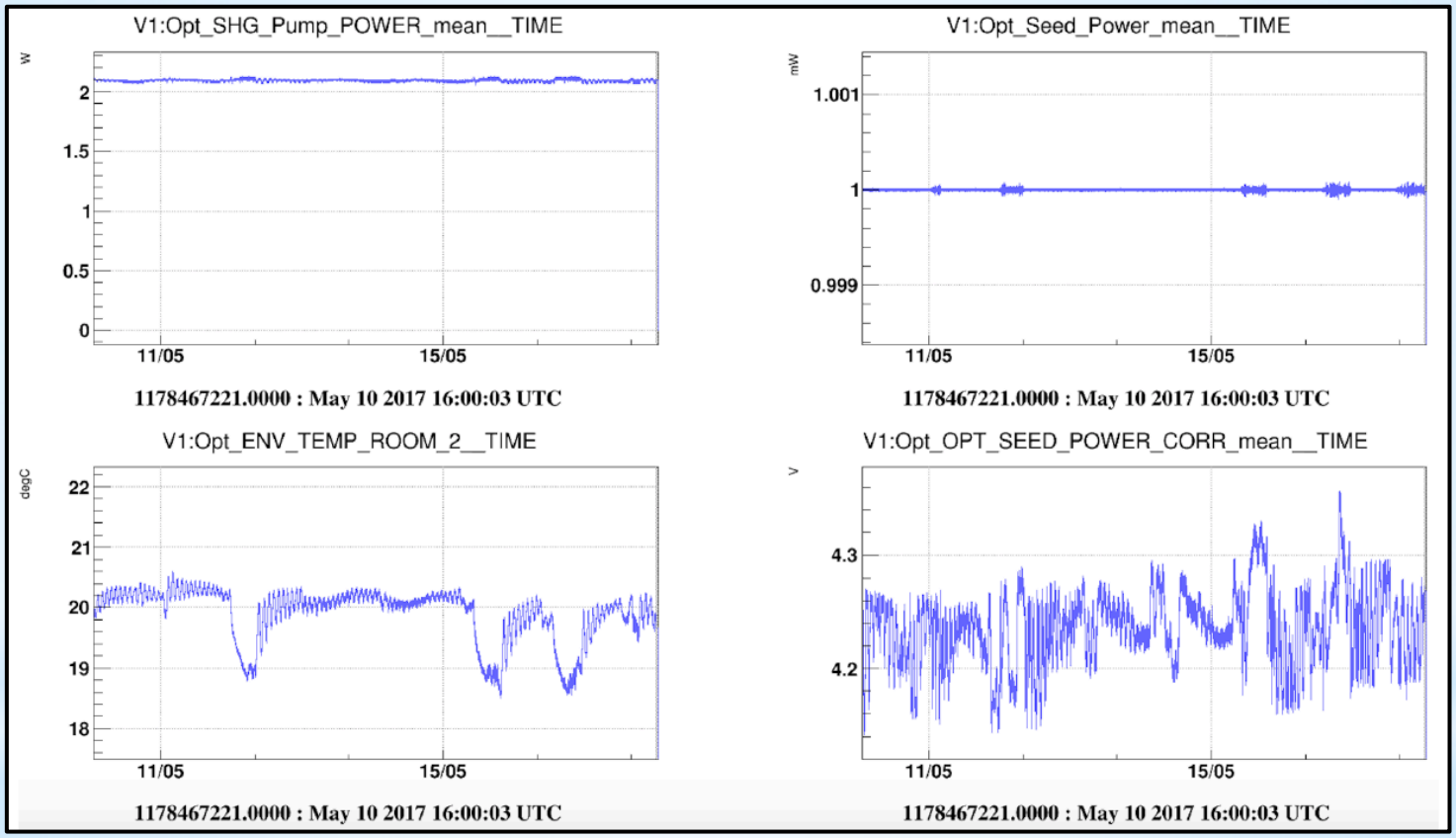

The long run power stability of IR laser source at 1064 nm. The data is acquired over 5 days and this measurement was performed with 2 W fiber amplifier.

Credits G. Pillant

Portability of the system

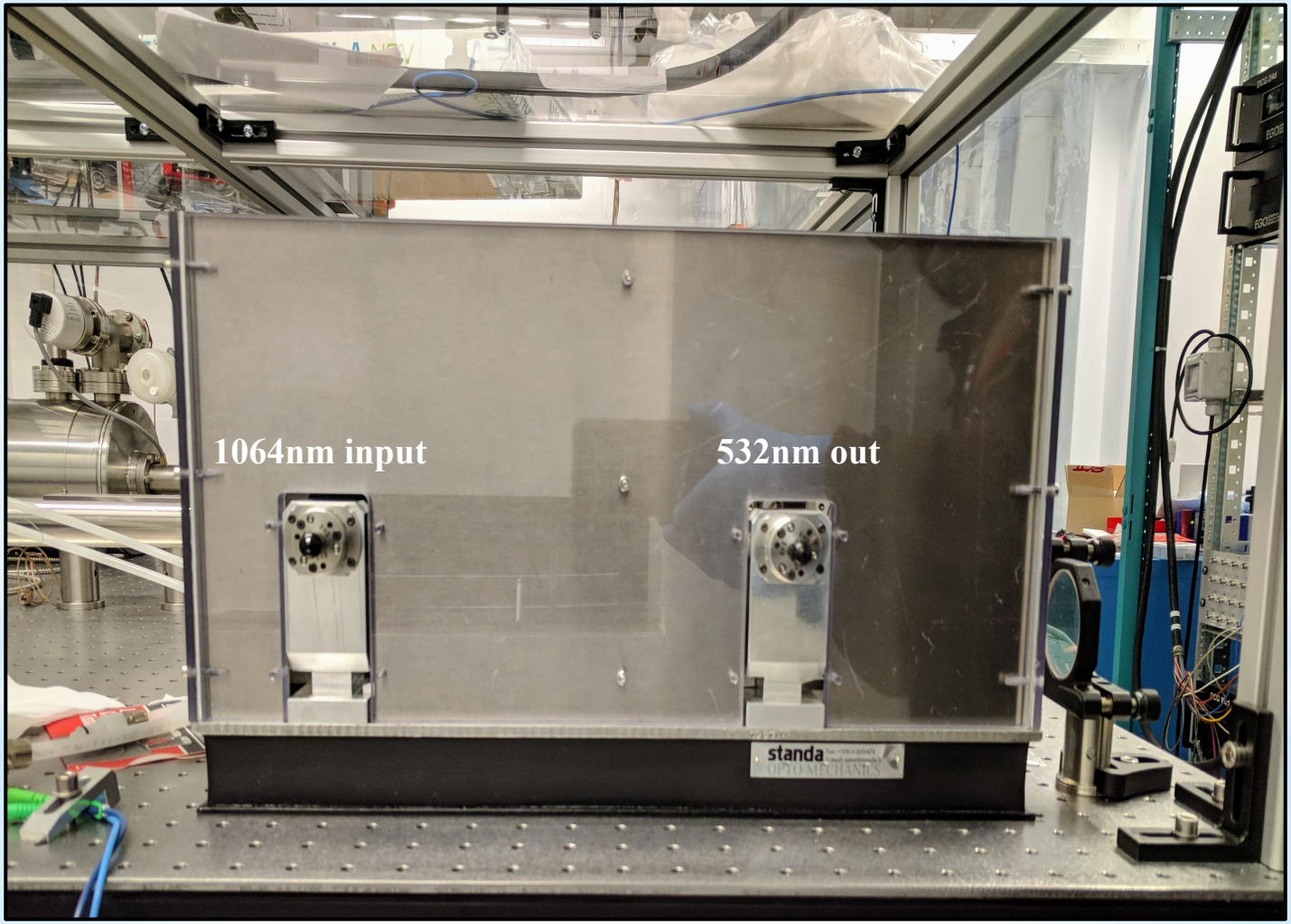

Auxiliary lasers in AdV: Conceptual scheme

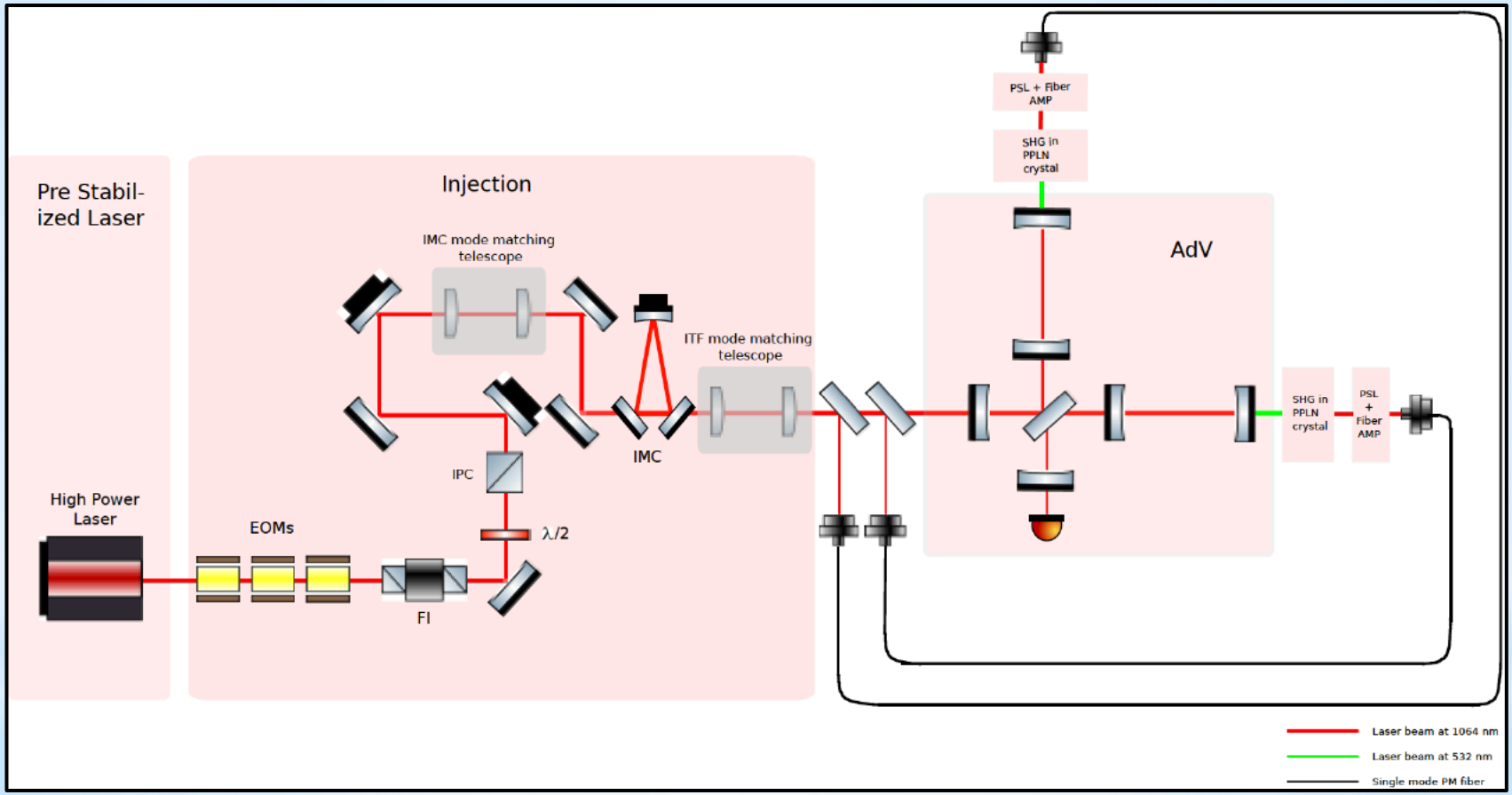

Fibered amplified IR laser source at 1064 nm using seed laser beams at 1064 nm from AdV injection subsystem. This conceptual scheme excludes all the control schemes representations, required in the injection susbsystem to implement control signals for EOMs, PZT mirrors, and optical cavities for the sake of simplicity. Here the PSL stands for pre-stabilized laser.

Phase Noise characterization of Fibered Amplified IR Laser source

1. Koheras BOOSTIK-Y10-5W **(5 W)**
2. KEOPSYS CYFA-PB **(2 W)**

Phase noise

Idea signal

$V(t)= A_0 \sin(\omega_0 t)$

Where,

A_0: Nominal amplitude

ω_0: Nominal frequency

Real life signal

$V(t)= (A_0+E(t)) \sin(\omega_0 t+\phi(t))$

Where,

E(t): Random amplitude fluctuations

$\phi(t)$: Random phase fluctuations

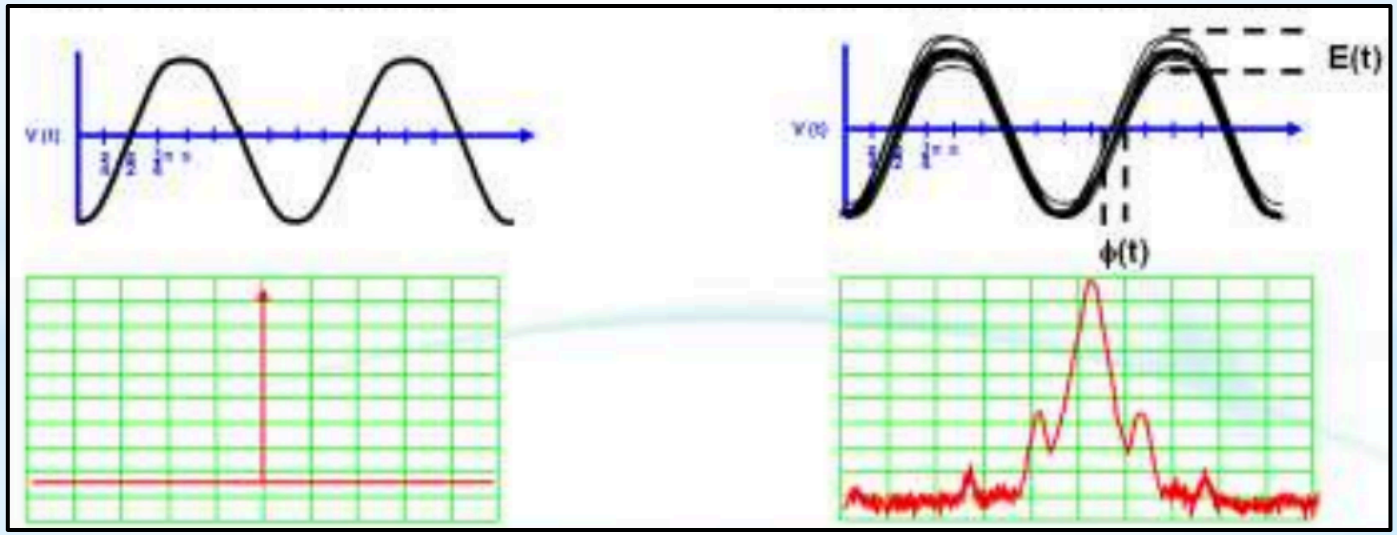

Credits: Agilent technologies

Beatnote between two laser fields

Requirements on the measurement:

- The spectrum analyzer phase noise must be lower than the noise at the offset frequency of the source under test.
- The amplitude noise of the source under test must be well below its phase noise.

The direct phase noise measurement method provides a quick way to check the noise of the system, though it is limited by the dynamic range of the spectrum analyzer.

$$I_{BN} = | E_1 \cos(w_1 t) + E_2 \cos(w_2 t) |^2$$

$$I_{BN} = E_1^2 \cos^2(w_1 t) + E_2^2 \cos^2(w_2 t) + 2E_1 E_2 \cos(w_1 t) \cos(w_2 t)$$

$$I_{BN} = 2E_1 E_2 \cos(w_1 t) \cos(w_2 t)$$

$$I_{BN} = E_1 E_2 [\cos(w_1 + w_2)t + \cos(w_1 - w_2)t]$$

$$I_{BN} = E_1 E_2 [\cos(w_1 - w_2)t]$$

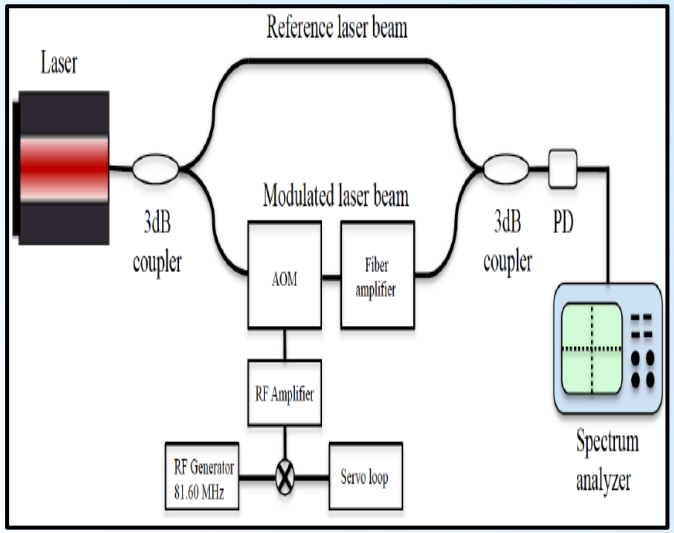

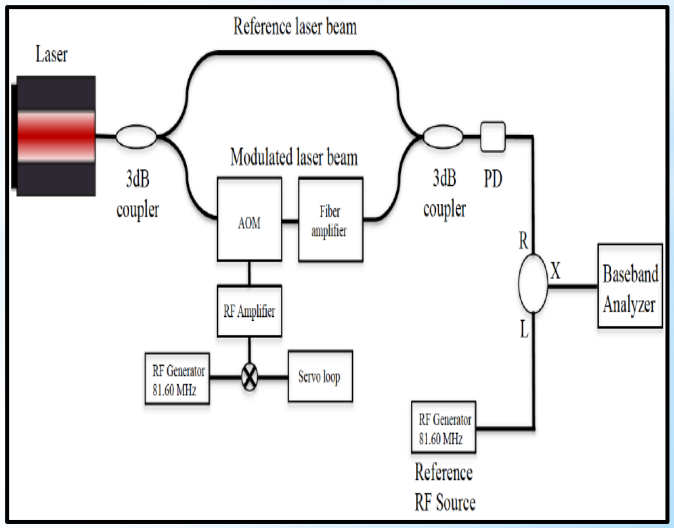

Power Spectral Density of 2W vs 5W fiber amplifier

Frequency span: 10 kHz

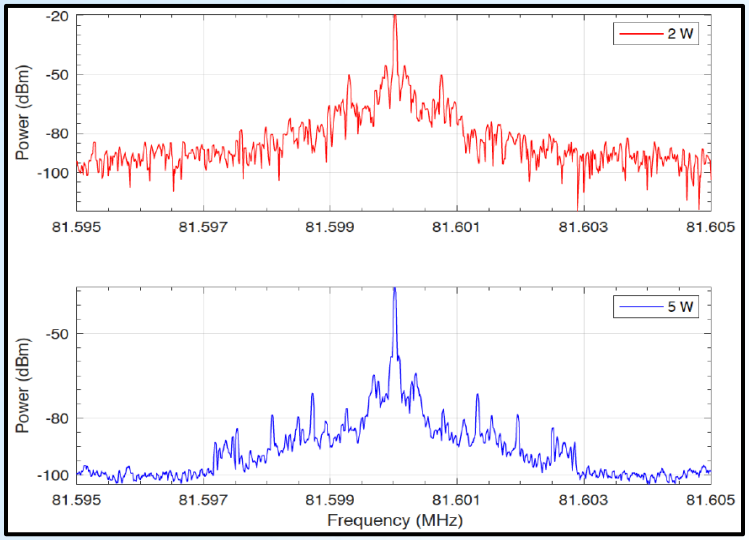

Observation:

KEOPSYS CYFA-PB (2 W) fiber amplifier offers less noise in the low frequency bandwidth compared to Koheras BOOSTIK-Y10-5W (5 W) fiber amplifier

Frequency span: 100 kHz

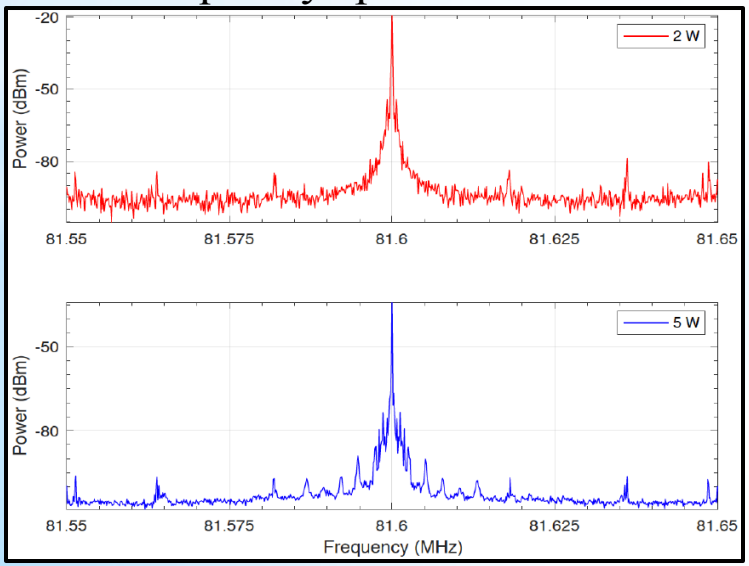

Frequency span: 500 kHz

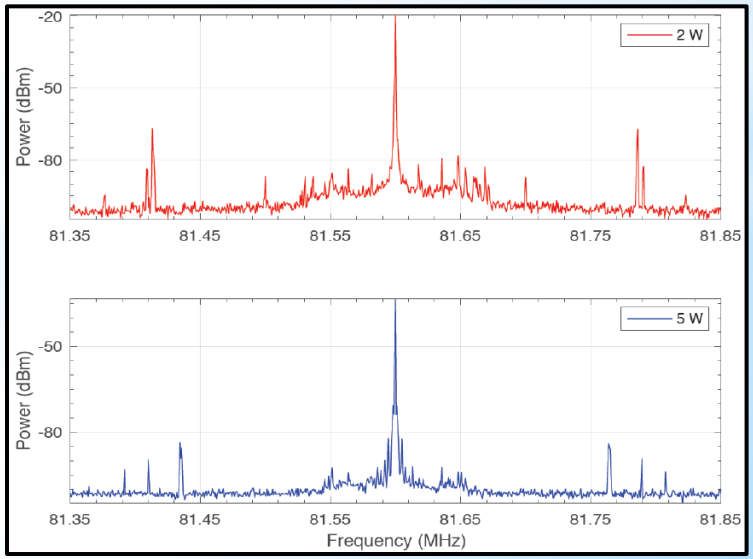

Single Side Band (SSB) noise

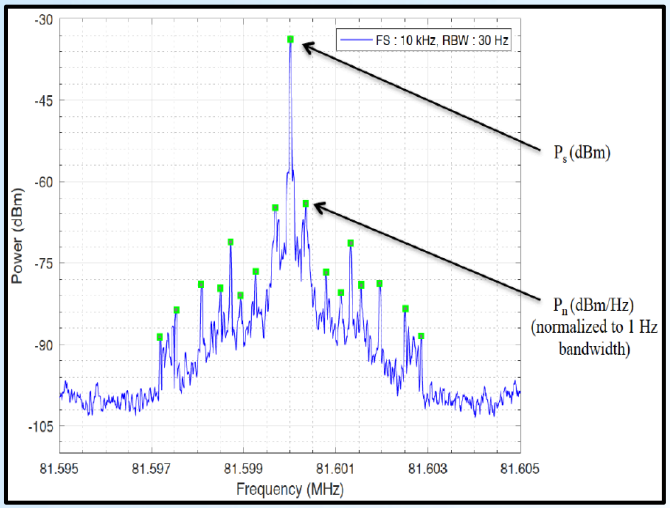

$$\mathcal{L}(f) = \frac{\text{Noise power in 1 Hz bandwidth}}{\text{Total signal power}}$$

$$\mathcal{L}(f) = \mathrm{P_n(dBm/Hz)} - \mathrm{P_s(dBm)}$$

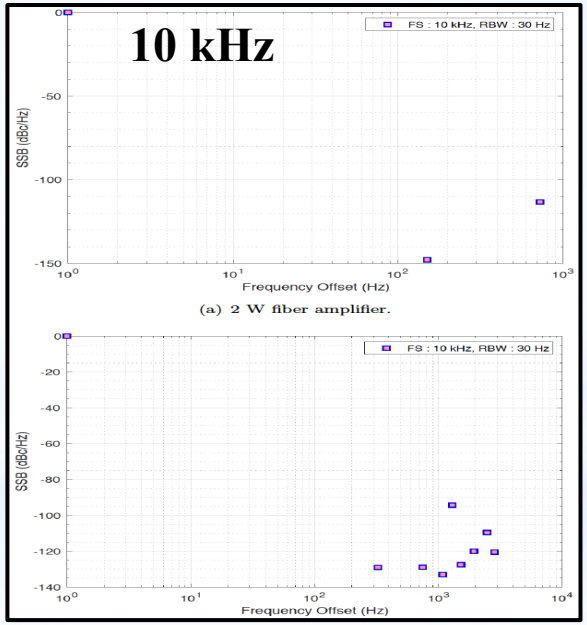

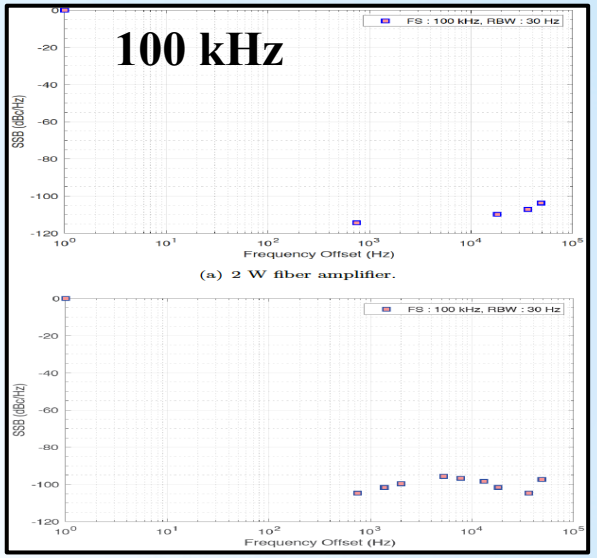

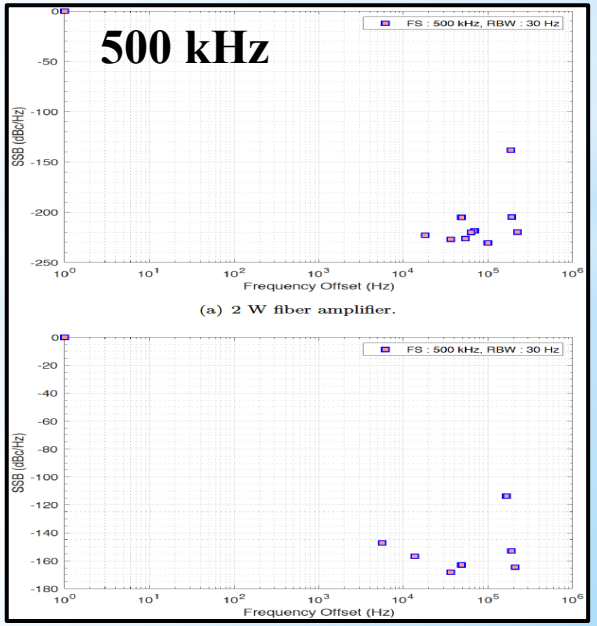

SSB measured at different frequency Spans i.e., 10, 100 and 500 kHz with RBW: 30 Hz.

Observation:
The measured SSB is mostly below 100 dBc/Hz for all the measurements.

BeatNote before PSL, after PSL and after SHG crystal

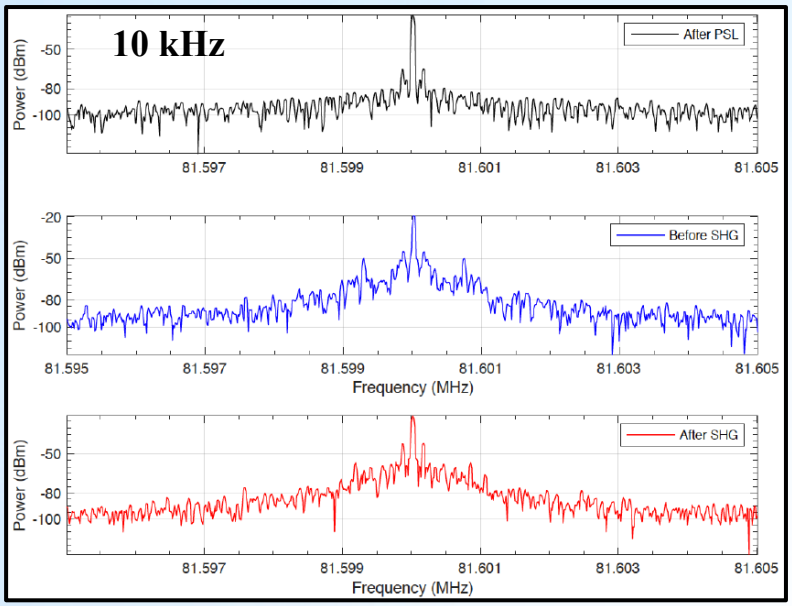

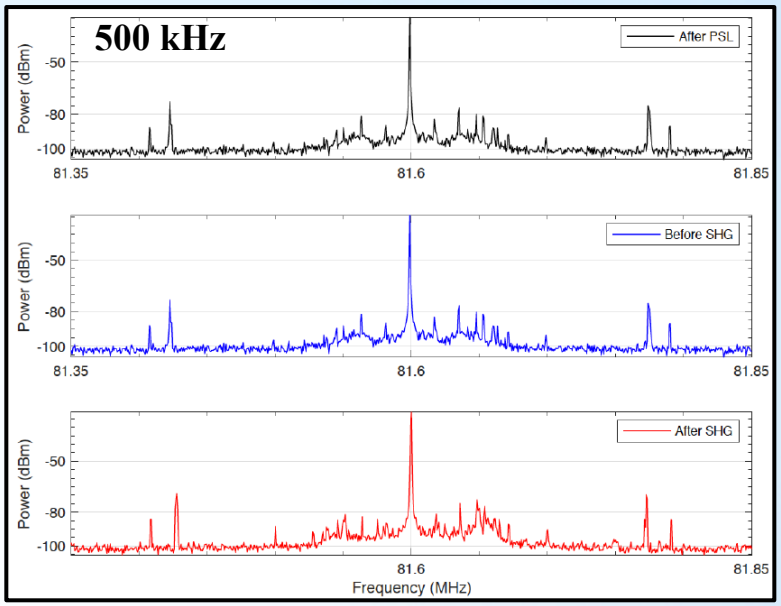

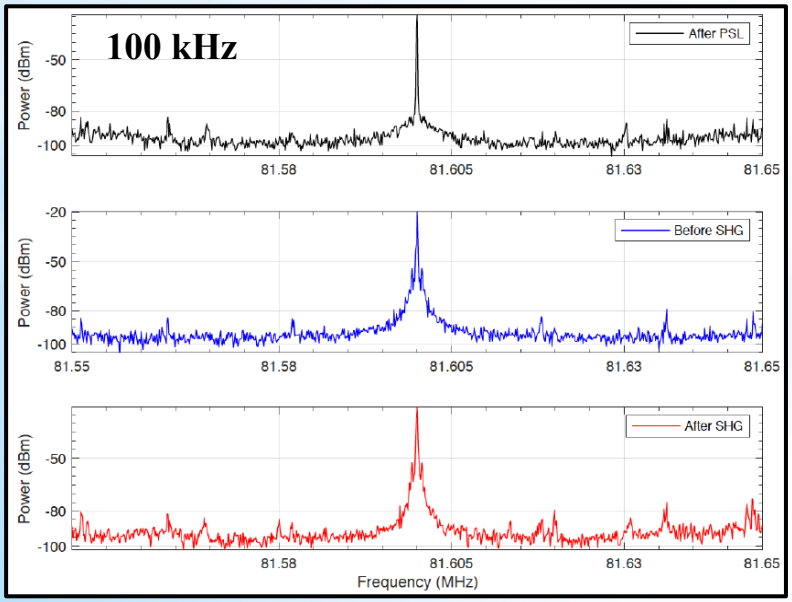

For all the three measurements with frequency Spans 10 kHz, 100 kHz and 500 kHz, we didn't observe additional noise added.

Observation:
We observed no additional offset frequencies in the system after PSL, before SHG and after SHG.

Beatenote measurement using demodulating technique (5 W fiber amplifier)

In the demodulating technique, the already obtained beatnote is demodulated such that, we see the beatnote in the detection bandwidth of AdV.

Observation:

The recorded beatnote signal before after PSL, before SHG and after SHG shows that the offset frequencies appearing are only amplified

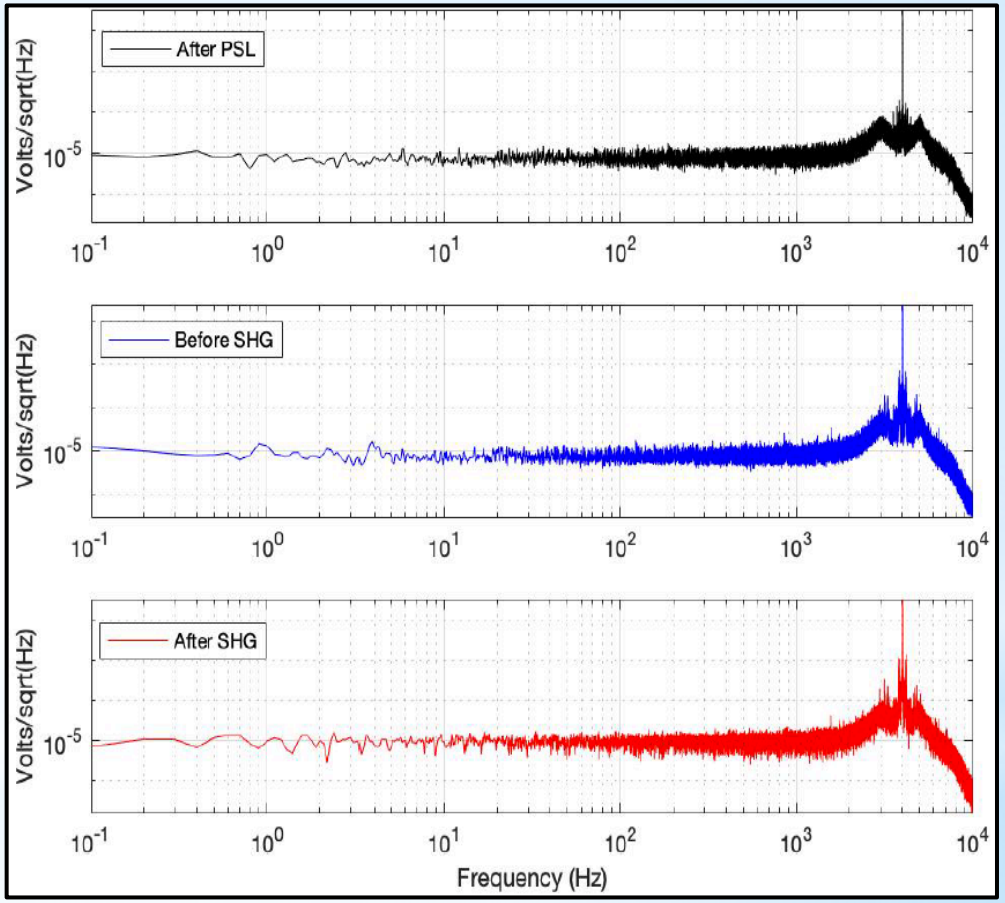

Beatnote measurement using demodulating technique. We demodulated the beatnote at 81.6 MHz+4.5 kHz, and acquired it using the data acquisition system of Virgo detector.

Squeezed states of light light generation experiment

Squeezing Experiment

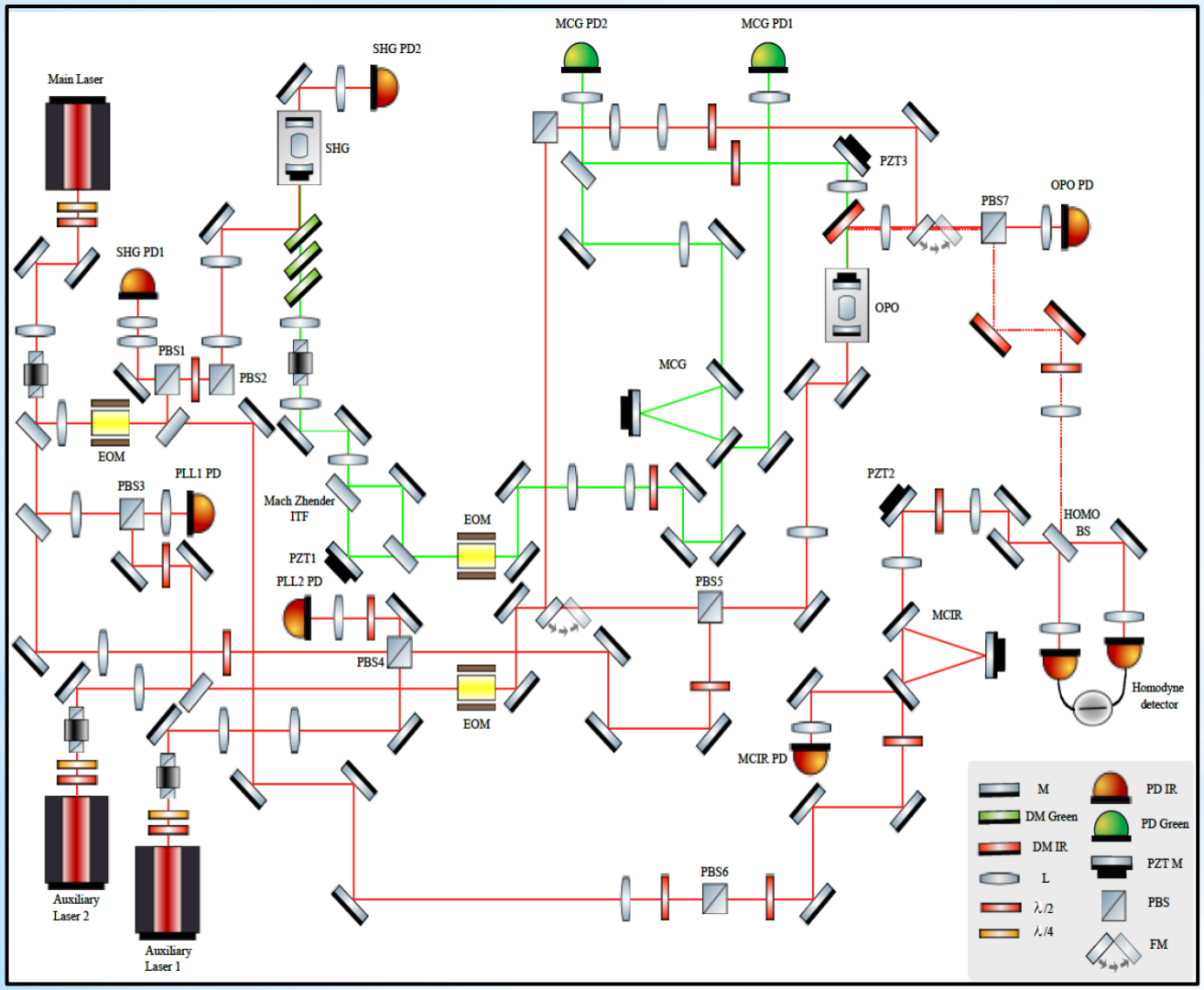

Optical layout of the squeezing experiment

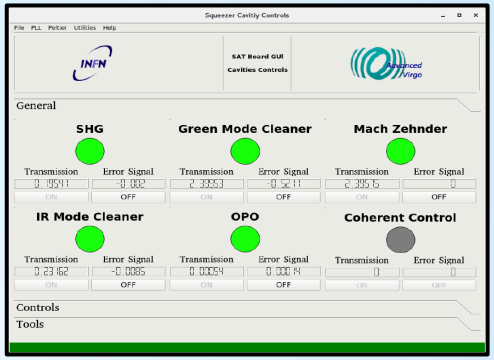

Control interface

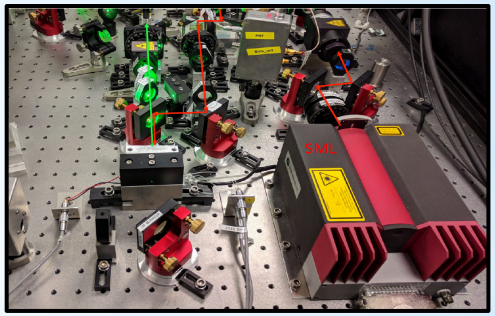

Main laser source

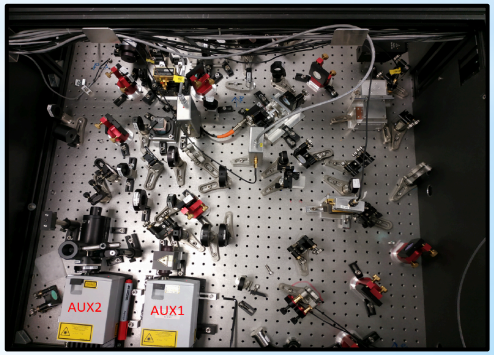

Auxiliary lasers

Phase locking of the laser sources

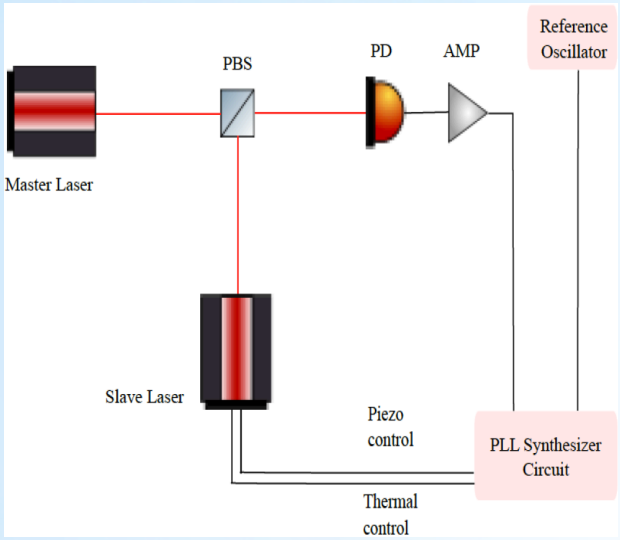

Feedback control system:
SL follow ML frequency variation

Input

- The **beat of the two lasers**
- A stable reference signal

Output

PID (Proportional integral derivative) control

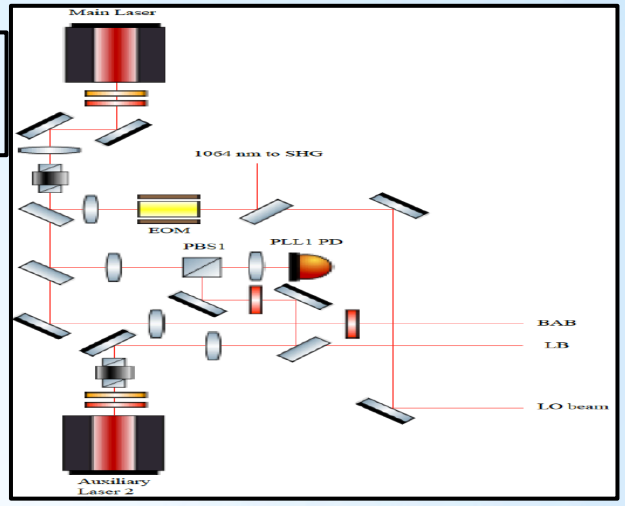

OPLL1

Slow control: Peltier cell (crystal refractive index change), bandwidth of 0-0,1 Hz

Fast control: Piezo-Electric Transducer (laser cavity length change), bandwdth up to kHz

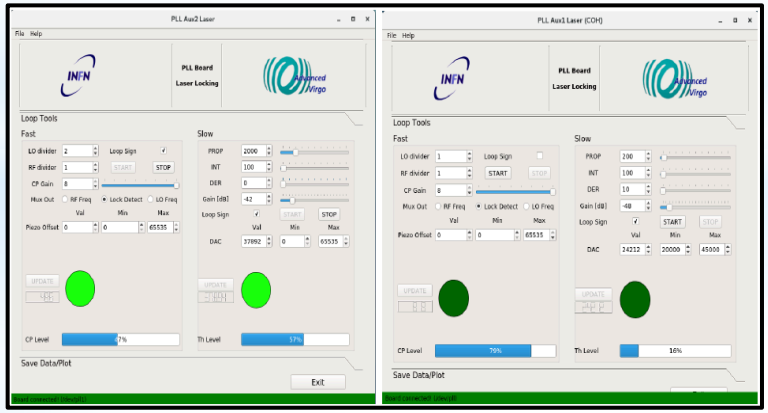

Control interface for OPLL

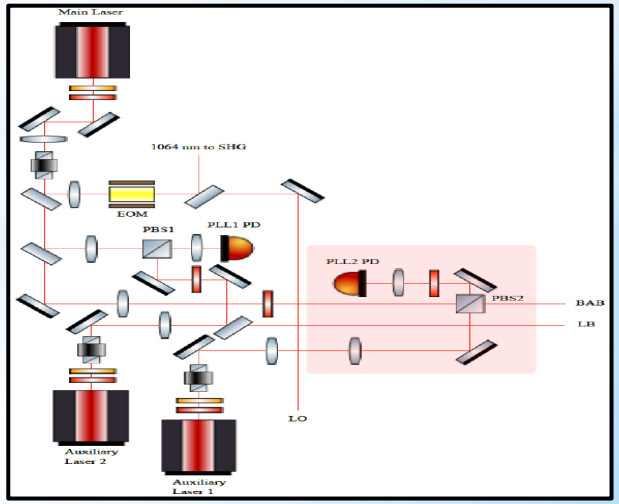

OPLL2

Pump beam generation

In-cavity SHG: a Fabry-Perot cavity that consists of a meniscus mirror and the PPKTP crystal (dimension: 1mm ×1.5mm ×9.3 mm).

Mode matching of 1064 nm: 98 %
Phase matching temperature: 31.6 °C
SHG conversion efficiency: more than 60 %

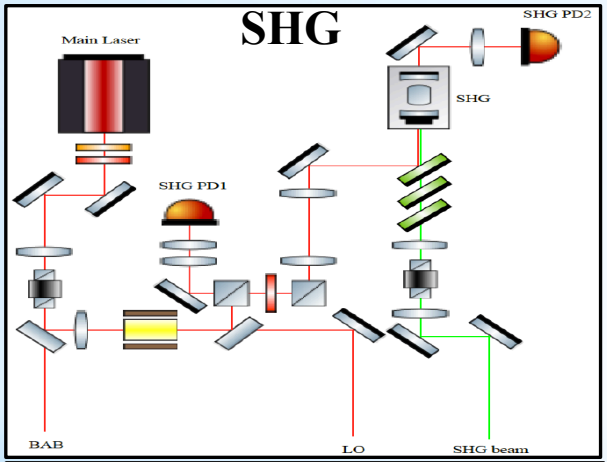

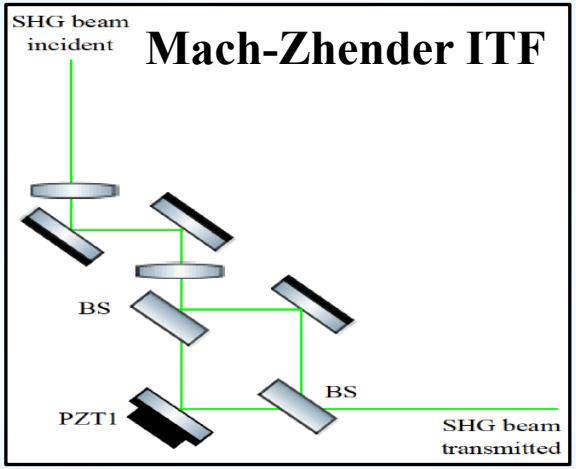

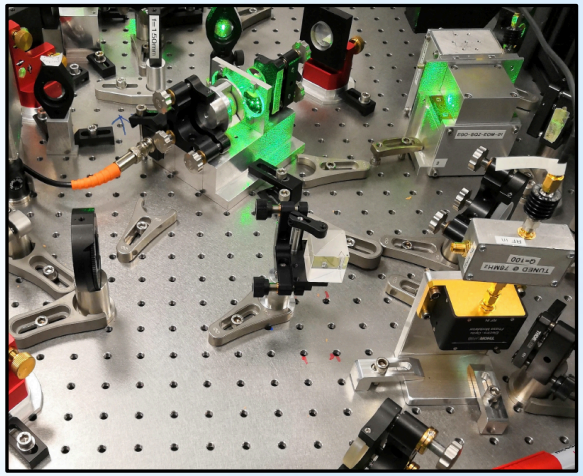

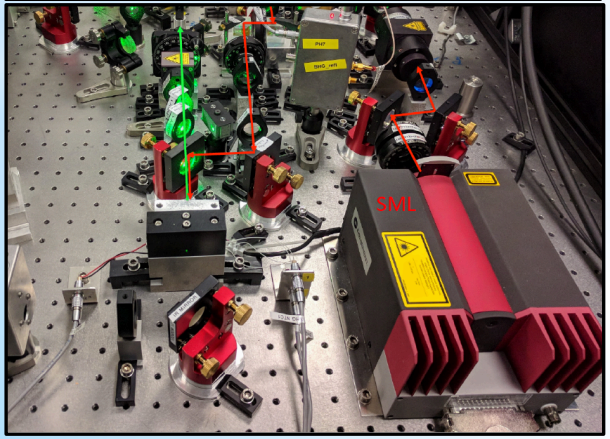

Long-term instability of the pump power

Spectral properties of SHG at 1064 :
Finesse is (**F** = 54),
Free Spectral Range (FSR) : 3.8 GHz
Full Width at Half Maximum (FWHM) : 71 MHz

Squeezing level degradation

Pump power stabilization within **1%**

Squeezing generation cavity: Optical Parametric Oscillator (OPO)

Geometrical properties

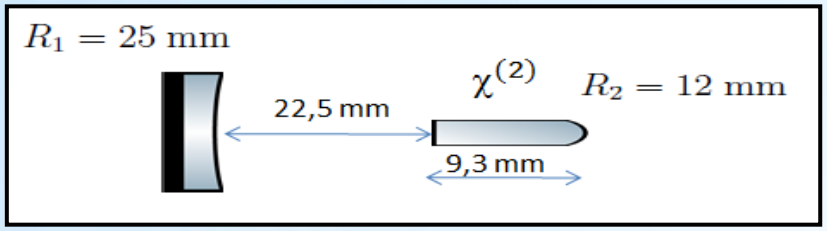

Goal: 13 dB generated squeezing

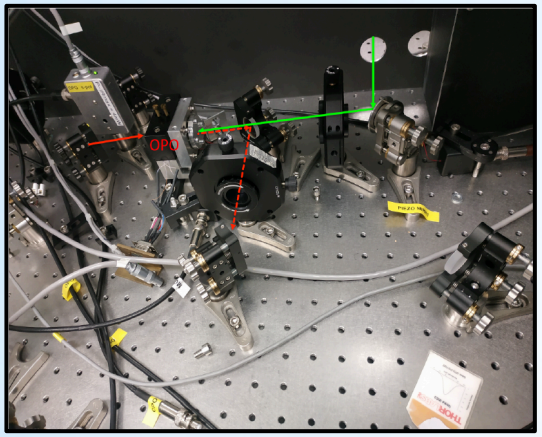

Co-resonance of the LB and BAB on OPO.

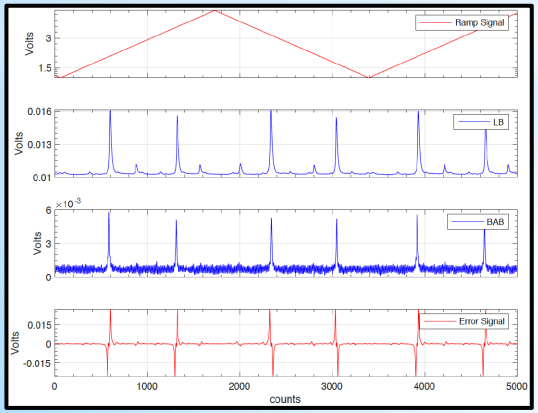

Parametric gain OPO

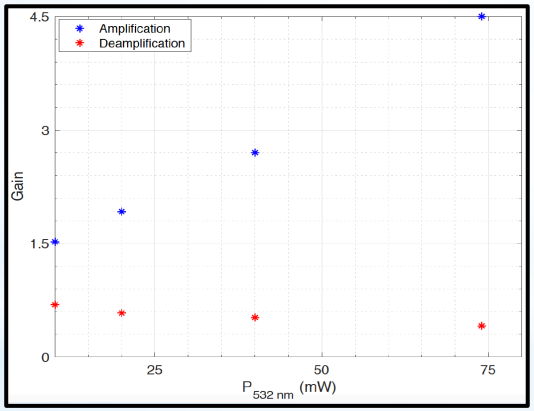

The parametric interaction in OPO leads to amplification and deamplification of the signal field.

Spectral properties of OPO cavity

OPO interaction: singly-resonant OPO cavity
- Less pump power absorption
- Absence of intra-cavity dispersion

λ nm	R_{cp} -	R_{pl} -	R_{cr} -	FSR GHz	FWHM MHz	$\mathcal{F}$ -
1064	0.92	< 0.02	> 0.99	3.80	50	75
532	0.20	<0.02	> 0.99	3.74	1.01	3.7

IR Power Reflectivity	Squeezing Level [dB]	Finesse
90%	-13.58	59.4
91%	-13.25	66.29
92%	-12.88	74.9

With an IR power reflectivity of 92% it is possible to have the maximum value of Finesse (upto produce roughly 13 dB of squeezing). Calculations performed using a ratio between pump power and threshold power equal to 0.64

Losses in squeezing measurement

$$V_+^{meas} = \eta V_+^{prod} + (1 - \eta)$$

where $\eta = 1 - Loss$

is the measurement efficiency, that includes the propagation efficiency, the photodiode quantum efficiency and the homodyne detection efficiency.

Homodyne detector

Measures difference in photocurents

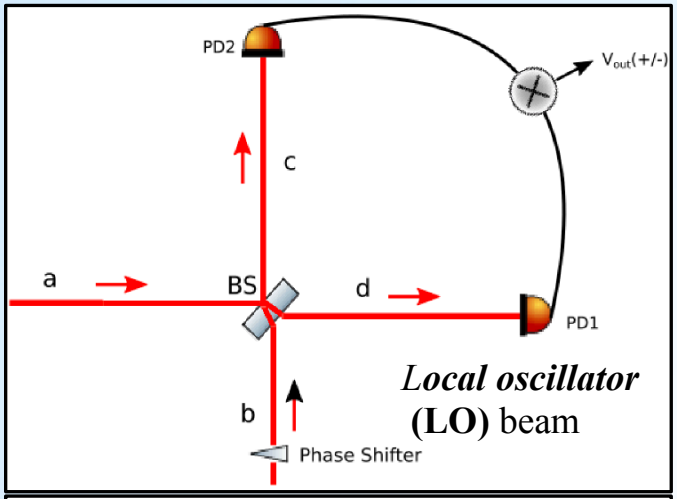

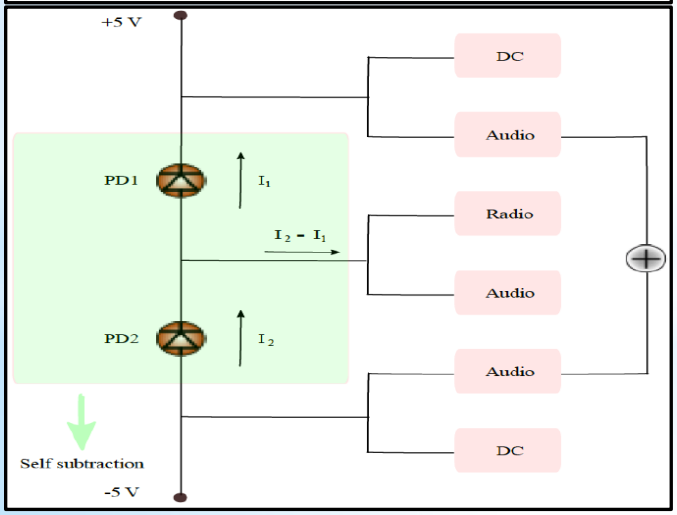

Conceptual scheme of the homodyne circuit. The acquired difference in photocurrents is readout in two different bandwidths i.e., Audio channel (10 Hz to 10 kHz) and the RF bandwidth (1 MHz to 120 MHz).

Main factors that limit homodyne performances:

- Beam Splitter not perfectly 50:50
- Light Scattering
- Beam Jitter
- Mode Shape changes
- Phase Jitter
- Electronic components unbalance

Efficient homodyne detection
needs the squeeze and the LO beams
To have:

- same frequency
- same spatial mode
- same polarization

Fringe visibility

$$\mathcal{V} = \frac{V_{max} - V_{min}}{V_{max} + V_{min}}$$

Homodyne detector characterization

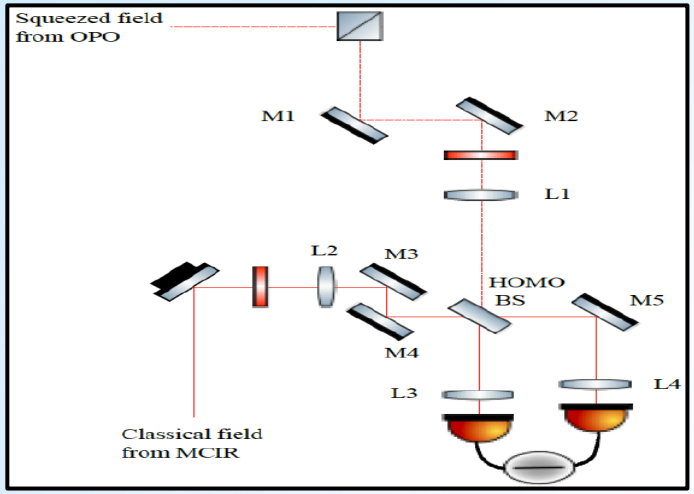

Homodyne characterization optical layout

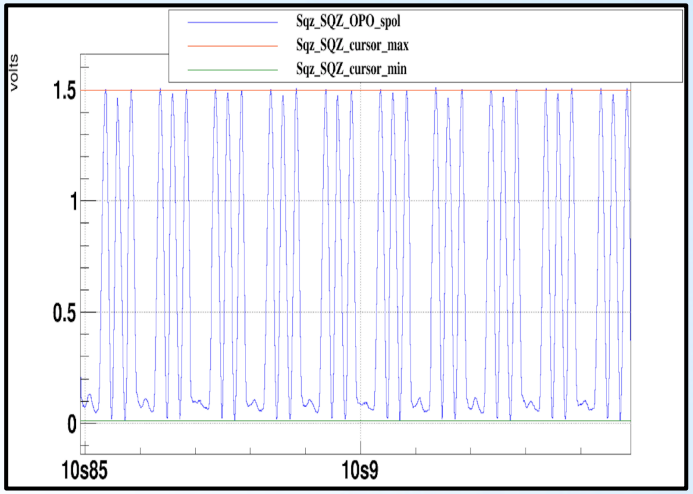

Fringe visibility between LO and squeezed field

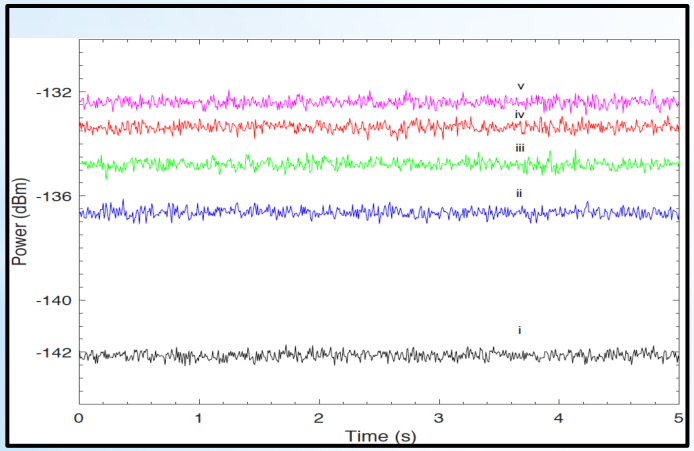

Linearity and clearance of the balanced homodyne detector. (i) is electronic noise level, (ii) is shot noise level at 1 mW, (iii) is shot noise level at 1.7mW, (iv) is shot noise level at 2.5 mW and (v) is shot noise level at 3.24 mW of LO laser field.

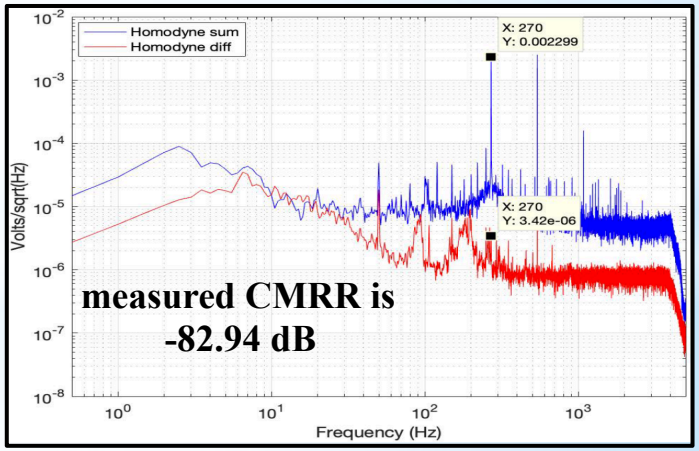

CMRR measurement. The modulation peak at 270 Hz can be seen in the sum, while it is minimized in the difference channel.

Squeezing measurement

4 dB measured squeezing

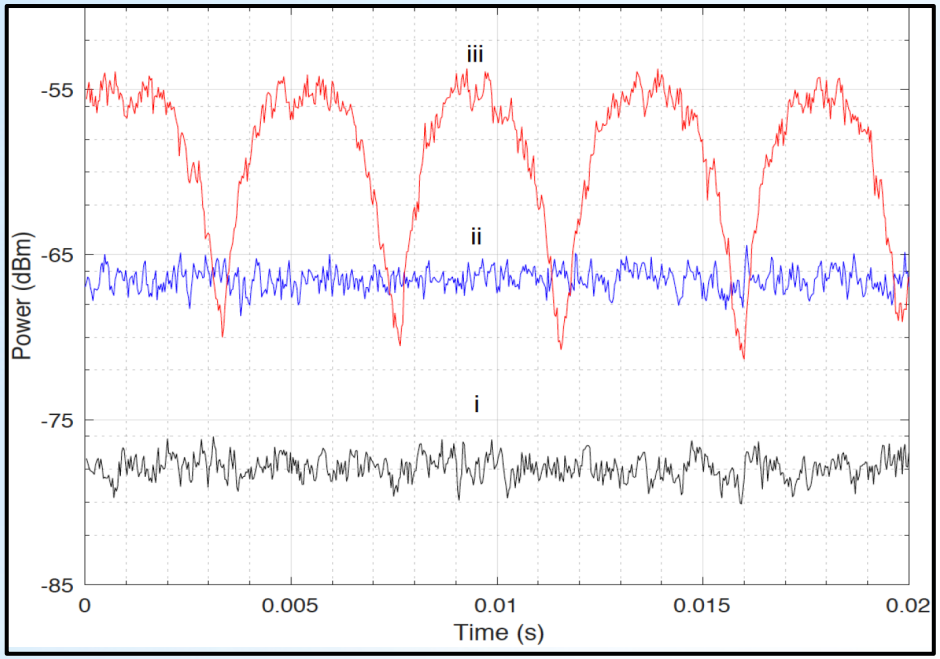

Preliminary squeezing measurement in the radio frequency band. The characterization is performed at 1MHz of Fourier frequency with 300 kHz of RBW and a time window of 20 ms is set on the spectrum analyzer. The three traces in the figure are categorized as: trace (i) is the homodyne dark noise, trace (ii) is the LO shot noise and the trace (iii) is the squeezing injected reduction and enhancement of the shot noise level of LO field.

Work in progress:
Coherent control scheme implementation

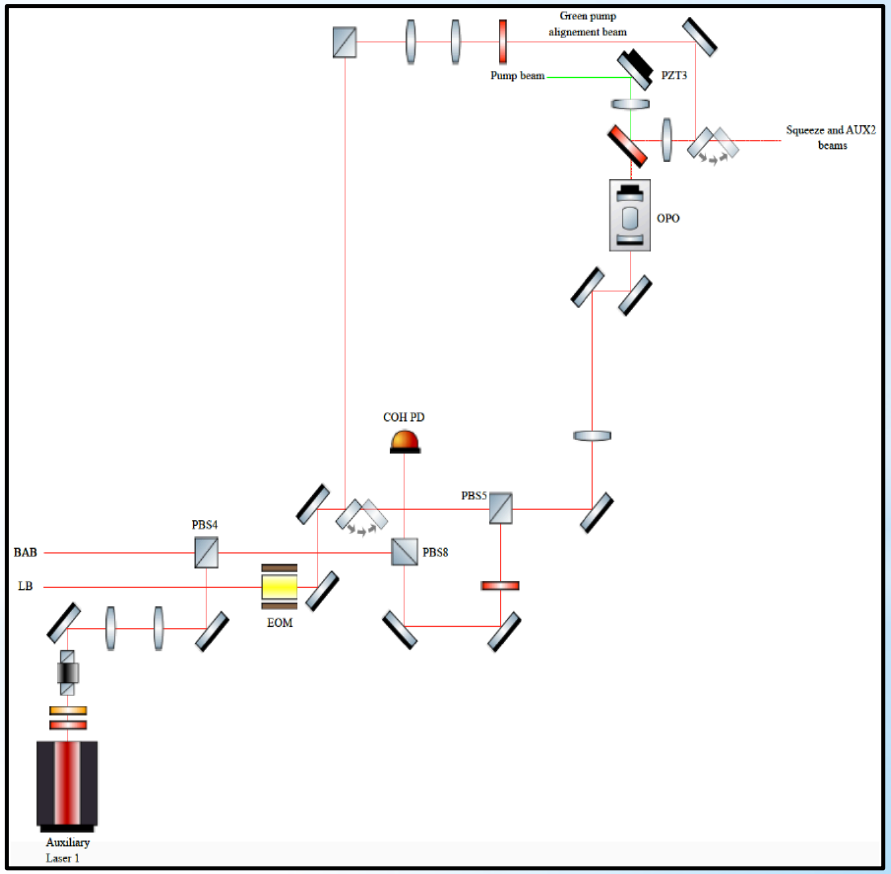

Conclusion

* Brief introduction about Gravitational Waves is presented.
* The thesis argument aims at quantum noise limited interferometric measurements.
* Three experimental activities have been performed over the course of PhD thesis work.
* Single pass SHG in PPKTP crystal to be possibly used as alternate to in-cavity squeezing pump beam generation
* Single pass SHG in PPLN crystal to be possibly used as AdV auxiliary lasers.
* Squeezed states of light generation experiment. Optical characterization of the bench is presented with preliminary squeezing measurement in the RF bandwidth. The bench will be used for the EPR squeezing (an alternate to filter cavity based frequency dependent squeezing) experiment

List of attended schools

1. A one week school, addressed to PhD students and young post-docs in scientific disciplines, focused on gravitational wave data analysis held between 9-15 November 2015 at the Gran Sasso Science Institute (GSSI), in L'Aquila, by the GraWIToN European consortium.
2. A one-week long school, addressed to PhD students and young post-docs focused on different aspects of gravitational wave research: Optics, Simulation, High Power Lasers and Data Analysis) held between 25-29 January 2016 at the Gravitational Wave Group, University of Birmingham.
3. A one week school held between 12-16 September 2016 at Max Planck Institute for Gravitational Physics on Optics, Simulation, High Power Lasers and Data Analysis, Hannover Germany.
4. A one week school on Project Management and Communication held between 21-25 November 2016 at EGO - European Gravitational Observatory, Cascina Italy.

List of attended conferences/meetings/workshops

1. A one week workshop "GWADW2016 - Impact of Recent Discoveries on Future Detector Design" in La Biodola, Isola d'Elba, Italy organised by GWIC , the Gravitational Wave International Committee held between 22-28 May 2016.
2. A one week long LIGO-Virgo meeting to discuss the current and future prospects and challenges in Gravitational Waves astronomy held between 28 August to 1 September 2017 at CERN, Switzerland.
3. A one week long Annual conference of the IEEE Photonics Society IPC on optical technologies held between 30 September to 4 October 2018 in Reston, VA, USA.
4. Bi-annual Virgo week organized at Virgo site, where the Virgo scientists present their work and discuss the challenges and advancements of AdV detector.

List of talks/posters presented at conferences/meetings/workshops

1. Bawaj M., Bazzan M., Calloni E., Conti L., Dattilo V., De Laurentis M., Di Pace S., Fafone V., Khan I., Genin E., Gemme G., Gennai A., Leonardi., Majorana E., Naticchioni L., Nocera F., Paoletti F., Passuello D., Pegoraro M., Perciballi M., Pillant G., Prevedelli M., Prodi G., Ricci F., Rocchi A., Sequino V., Sorrentino F., Vardaro M., Zendri J.P., Development of an audio-frequency band vacuum squeezer for the quantum noise reduction in the Gravitational Wave detector Advanced Virgo, Poster presented at 12th Amaldi Conference, Pasadena, CA (US) 9-14 July, 2017.

2. M. Bawaj, M. Bazzan, E. Calloni, L. Conti, M. De Laurentis, S. Di Pace, V. Fafone, J. Harms, I. Khan, G. Gemme, A. Gennai,E. Majorana, L. Naticchioni, D. Passuello, G. Prodi, F. Ricci, A. Rocchi, V. Sequino, F. Sorrentino, M. Vardaro, J. P. Zendri, Application of EPR entanglement for frequency dependent squeezing in
Advanced Virgo, Poster presented at LSC-Virgo meeting 2017 at CERN, August 28- September 1, 2017, Geneva, Switzerland.

3. Khan I., Fafone V., Genin E., Karan K., Pillant G., Rocchi A., Sequino V., Vahlbruch H., Generation of green pump source from a PPKTP crystal in single pass SHG conguration for Squeezing experiment, Poster presented at LSC-Virgo meeting 2017 at CERN, August 28- September 1, 2017, Geneva, Switzerland.

4. M. Vardaro, M. Bawaj, M. Bazzan, F. Bergamin, E. Calloni, G. Cerretani, L. Conti, V. Dattilo, M. De Laurentis M., S. Di Pace, V. Fafone, I. Khan, G. Gemme, A. Gennai, M.Leonardi, E. Majorana, L. Naticchioni, F. Nocera, F. Paoletti, D. Passuelo, M. Pegoraro, G. Pillant, M. Prevedelli, G. A. Prodi, F. Ricci, A. Rocchi,
V. Sequino, F. Sorrentino, J. P. Zendri, A fully automated and digitally controlled squeezed vacuum source, Poster presented at LSC-Virgo meeting 2017 at CERN, August 28- September 1, 2017, Geneva, Switzerland.

5. Barsuglia M., Bawaj M., Bazzan M., Calloni E., Conti L., D?Angelo B., De Laurentis M., De Rosa R., Di Pace S, Fafone V., Garaventa B., Gemme G., Gennai A., Giacoppo L., Harms J., Khan I., Majorana E., Naticchioni L., Nguyen C., Passuello D., Prodi G., Ricci F., Rocchi A., Sequino V., Sorrentino F., Vardaro M., Zendri J.P., Reducing quantum noise for Advanced Virgo gravitational-wave detector by using frequency-dependent squeezing technique with Einstein-Podolsky-Rosen (EPR) entanglement, at GWADWWorkshop 2019, Isola d' Elba, Italy 19-25 May 2019.

6. Oral presentation on "Fibered amplied Infrared laser source at 1064 nm for the generation of Auxiliary Lasers at 532 nm for Advanced Virgo detector" to be held between 19-21 June 2019 at the 10th Young Researcher Meeting in Rome.

List of publications

1. Conference proceeding on "*Auxiliary lasers for Advanced Virgo Gravitational Waves detector using single pass Second Harmonic Generation in Periodically Poled Lithium Niobate crystal*", intended to be published in be published in Journal of Physics: Conference series is under review by **Virgo Editorial Board.**

2. Manuscript of intended journal publication entitles, "*Finite state machine controls for a source of optical squeezed vacuum*" is sunder progress within the squeezing work team.

3. List of LIGO-Virgo collaboration papers as enclosed in the PhD activity report submitted to GSSI.

Acknowledgements

* Prof. Viviana Fafone, Dr. Valeria Sequino, Dr. Fiodor Sorrentino, Dr. Martina Di Laurentis, Dr. Eric Genin, Mr. Gabriel Pillant, Dr. Henning Vahlbruch, Dr. Moritz Mehmet, Prof. Dr. Benno Willke, Prof. Eugenio Coccia, Dr. Michele Punturo, Dr. Alessio Rocchi, Dr. Elena and Ms. Erica.
* Colleagues (PP1 building), and all the support staff at INFN Tor Vergata section.
* Gran Sasso Science Institute, INFN, European Gravitational Observatory, and Albert Einstein Institute.
* Marie Curie ITN project GraWIToN.

Thank you ☺